

Survey of vector-like fermion extensions of the Standard Model and their phenomenological implications

Sebastian A.R. Ellis^{a*}, Rohini M. Godbole^{b†}, Shrihari Gopalakrishna^{c‡}, James D. Wells^{a§}

^a Physics Department, University of Michigan, Ann Arbor, MI, USA

^b Center for High Energy Physics, Indian Institute of Science, Bangalore, India

^c Institute of Mathematical Sciences (IMSc), Chennai, India.

November 17, 2014

Abstract

With the renewed interest in vector-like fermion extensions of the Standard Model, we present here a study of multiple vector-like theories and their phenomenological implications. Our focus is mostly on minimal flavor conserving theories that couple the vector-like fermions to the SM gauge fields and mix only weakly with SM fermions so as to avoid flavor problems. We present calculations for precision electroweak and vector-like state decays, which are needed to investigate compatibility with currently known data. We investigate the impact of vector-like fermions on Higgs boson production and decay, including loop contributions, in a wide variety of vector-like extensions and their parameter spaces.

*sarellis@umich.edu

†rohini@cts.iisc.ernet.in

‡shri@imsc.res.in

§jwells@umich.edu

Contents

1	Introduction	3
2	Vector-like-fermion Models	5
2.1	The $1\bar{1}$ Model	7
2.2	The $2\bar{2}$ Model	7
2.3	The $2\bar{2}(1\bar{1})_1$ Model	7
2.3.1	Υ Model	7
2.3.2	ξ Model	9
2.3.3	Alternate Yukawa coupling	10
2.4	The $2\bar{2}(1\bar{1})_2$ Model	10
2.5	Some vector-like Extensions of the SM	11
3	Precision Electroweak Observables	13
3.1	S, T, U Constraints	13
3.2	S, T, U in the $2\bar{2}(1\bar{1})_1$ model	14
3.2.1	Υ Model	14
3.2.2	ξ Model	15
3.2.3	Υ Model with alternate Yukawa coupling	15
3.3	S, T, U in the $2\bar{2}(1\bar{1})_2$ model	15
3.4	Shift in the $Zb\bar{b}$ coupling	15
4	Direct Collider Constraints	16
4.1	Mass and gauge eigenstates	16
4.2	Computation of decay widths	19
4.3	Experimental Limits from VLQuark searches	20
4.4	Experimental Limits from VLLepton searches	21
5	Higgs Production and Decay Processes	21
6	Numerical Results for Electroweak and Higgs Boson Observables	23
6.1	MVLE ₁ vector-like Leptons Model	24
6.2	MVQD ₁ vector-like Quarks Model	26
6.3	VSM ₁ vector-like Standard Model	26
6.4	Fit to the LHC Higgs data	31
7	Conclusions	35
A	Gauge boson 2-point functions with vector-like fermions	36
B	Explicit expressions for the mixing coefficients	38

1 Introduction

The Standard Model of particle physics is a chiral theory under the electroweak gauge symmetries, $SU(2)_L \times U(1)_Y$. It is for this reason that a condensing Higgs boson is needed to generate elementary particle masses. Non-chiral pairs of fermions, or mirror pairs f_q and $f_{\bar{q}}$ are able to achieve mass explicitly through the gauge-invariant bilinear interaction $m_f f_q^\dagger f_{\bar{q}}$. There is no reason why such pairs of vector-like fermions do not exist. The only question is what is their mass, since it is in this case not tied at all to electroweak symmetry breaking.

In the literature there are numerous examples of theories that require vector-like fermions in the spectrum. As with all cases, the mass scale is uncertain. In supersymmetric theories we know that there must be vector-like fermions in the spectrum, namely the Higgsinos. The Higgsinos form a vector-like pair of fermions with the same quantum numbers as the left-handed leptons and its conjugate. Naturalness requires the Higgsinos to be near the weak scale, although the precise mechanism that achieves this is the subject of rich theoretical analysis – one that we do not traverse here. A general thought does rise with this observation, and that is why not vector-like complements of all the other SM fermions?

Indeed, more fundamental theories, such as string theories and D-brane theories, often do give rise generically to vector-like states. For example, Dijkstra et al. [1] search the landscape of orientifolds of Gepner models for Standard Model-like vacua of three generations and find a plethora of models with vector-like complements of the Standard Model states. In D-brane constructions it is generic to get these extra vector-like states since the computation for chiral fermion representations involves identifying topological intersection numbers, whereas the vector-like states multiplicity is not confined to that, and there can be many more. The chiral content is the “left over” chiral fermions that are necessarily lighter because they cannot be paired up to receive mass without the Higgs boson.

Since all string theories can be related through dualities, it is not surprising, although not a priori necessary, that there would be generic presence of vector-like states in other constructions. Indeed, there are additional cases. For example, the ubiquity of vector-like states is manifest also in orbifold constructions of heterotic string compactifications [2]. In this case, more realistic models tend to produce vector-like complements of the down-type fermions, $\mathbf{5} + \bar{\mathbf{5}}$ in $SU(5)$ language.

Both string examples discussed may also give rise to vector-like states of other representations, and even ones of fractional electric charge (see e.g., [3]). Vector-like families are not motivated only by string theory considerations, but also lower energy constructions such as top-quark seesaw models [4, 5, 6], warped extra dimensions (see for example Ref. [7] and references therein), composite Higgs [8, 9, 10, 11, 12, 13], little Higgs theories [14, 15, 16, 17], and low-scale supersymmetry [18, 19, 20, 21, 22, 23, 24, 25]. Ref. [19] shows that the Higgs mass can be raised in supersymmetry by the addition of vector-like matter. Ref. [20] considers the addition of vector-like matter to improve the little hierarchy problem in the MSSM. Ref. [22, 23, 24, 25] consider the implications of gauge mediated supersymmetry breaking with vector-like matter. Refs. [26, 27, 28, 29] also deal with various aspects of vector-like fermions. There is also interest in vector-like states from a purely agnostic phenomenological inquiry to potentially better fit Higgs boson data [30, 31]. Again, these ideas give rise to vector-like SM complements and also new representations. The implications and phenomenology of these latter states is qualitatively different than vector-like complements of the SM states, and will be discussed elsewhere.

There have been many works that have appeared since the discovery of the Higgs attempting to explain the preliminary discrepancies. An example is the “simplified models” approach of Ref. [33]. Ref. [30] attempted to explain the discrepancies in the Higgs data (with limited statistics) prevailing

then with vector-like fermions having non-standard hypercharge assignments. Ref. [31], with a similar goal, introduces only vector-like leptons with SM hypercharge assignment. Refs. [34, 35] considers a vector-like lepton generation (including new SU(2) singlets) and the possibility of the electromagnetic charge neutral vector-like lepton being a dark matter candidate. They analyze precision electroweak bounds, modifications to Higgs observables and vacuum stability bounds for this extension. Ref. [35] also investigates baryogenesis and vacuum stability in this context.

More recently, Ref. [36] considers vector-like quarks with SM EM charges. Their analysis of the SU(2) doublet case differs from ours in the following respects: (a) we add new SU(2) singlet vector-like quarks motivated by replicating the SM structure, while they do not. The constraints from shifts to $Zb\bar{b}$ couplings on their model is very tight, while this will not apply in our case since we do not allow any significant Yukawa coupling between the new SU(2) vector-like doublet and SM singlets; (b) they only consider quarks while we include leptons also; (c) we include the recent LHC Higgs data while their study was done before the Higgs discovery. Refs. [37, 38] also have SM singlets only, not new vector-like singlets like we consider. Ref. [39] considers the modification to double Higgs production due to vector-like fermions in such a model.

Ref. [40] performs a model-independent analysis of the recent Higgs data, obtains preferred regions of the effective couplings, and interprets this in the context of vector-like fermions. Since the SU(2) representations of the fermions are left unspecified, electroweak precision constraints have not been applied. In our work we consider a few concrete SU(2) representations and do apply electroweak precision constraints. Refs. [41] also perform an effective operator analysis of the Higgs data. Refs. [19, 20, 23, 36] discuss collider searches after taking into account precision electroweak constraints. Ref. [42] takes into account precision electroweak constraints and considers the t' pair production followed by the $t' \rightarrow th$, $h \rightarrow \gamma\gamma, ZZ$ decay modes, while Ref. [43] considers $t' \rightarrow th$ in the multi- b -jets channel. Ref. [44, 45] evaluates precision electroweak and flavor constraints on top-partner vector-like quarks, and studies direct LHC signatures.

In the following sections of this paper, we shall not discuss further the underlying motivations, but study carefully the theory construction and phenomenological implications of vector-like SM complement states. The masses and couplings will be free parameters for us, except that we will generally confine ourselves to the case of vector-like states mixing weakly with SM states. This is not absolutely required, but we do it so as not to complicate our work with detailed flavor physics. The high-energy manifestations and searches are our primary consideration, including the impact of vector-like states on the Higgs branching fractions, particularly into two photons. Since the mass of the vector-like fermions are not generated through the Yukawa couplings, the loop contributions involving the Higgs decouple faster than for chiral fermions. Hence the constraints from the current Higgs data, precision electroweak observables and direct searches are less severe for vector-like fermions than for chiral fermions.

To begin we develop a formalism for vector-like fermion models. In this work we identify properties of vector-like fermions that are consistent with the recently measured Higgs production cross-section and its decay branching ratios at the LHC. In particular, we analyze vector-like extensions of the Standard Model (VSM), with vector-like quarks and leptons. We investigate the precision electroweak constraints from their presence and then the direct collider constraints from LHC searches. We present many numerical results, which will have implications for future vector-like fermion searches. And we conclude with a brief discussion on the meaning of the results in the context of some theories of physics beyond the SM, and also discuss what the future may hold in our search for vector-like states.

2 Vector-like-fermion Models

We add to the SM a vector-like pair of $SU(2)$ doublets and some number of vector-like pair of $SU(2)$ singlets. We assume all these fields to be charged under $U(1)_Y$. Consider the vector-like doublets as two Weyl spinors χ_α and χ_α^c , that transform as conjugates with respect to $SU(2)_L$ and $U(1)_Y$, namely $\chi = (2, Y_\chi)$, $\chi^c = (\bar{2}, -Y_\chi)$. Although we are considering only one such doublet pair, one can add any number of such pairs and our statements below can be extended to include this case. The theory can equivalently be written in terms of a Dirac fermion

$$\mathcal{X} \equiv \begin{pmatrix} \chi_\alpha \\ \chi^{c\dot{\alpha}} \end{pmatrix},$$

where we follow the usual Lorentz index conventions $\alpha, \dot{\alpha}$. Thus the Dirac spinor \mathcal{X} transforms the same way as χ under $SU(2)_L$ and $U(1)_Y$. A vector-like mass term can always be added

$$\mathcal{L} = -M_\chi \chi \chi^c + h.c. = -M_\chi \bar{\mathcal{X}} \mathcal{X}. \quad (1)$$

Let us consider a vector-like pair of Weyl spinors $\chi = (2, Y_\chi)$, $\chi^c = (\bar{2}, -Y_\chi)$. Expanding the $SU(2)$ structure we can write

$$\chi = \begin{pmatrix} \chi_1 \\ \chi_2 \end{pmatrix}, \quad \text{or equivalently,} \quad \mathcal{X} = \begin{pmatrix} \mathcal{X}_1 \\ \mathcal{X}_2 \end{pmatrix},$$

where \mathcal{X} , \mathcal{X}_1 and \mathcal{X}_2 are Dirac fermions.

The W^3 and B interactions to new vector-like fermions have the structure

$$\mathcal{L} \supset \sum_i [g W_\mu^3 (T_{ii}^3) + g' B_\mu Y^i] [\bar{\mathcal{X}}_L^i \gamma^\mu \mathcal{X}_L^i + \bar{\mathcal{X}}_R^i \gamma^\mu \mathcal{X}_R^i], \quad (2)$$

with the W^3 also coupling to \mathcal{X}_R . The vector-like nature is exhibited by the L, R chiralities having the same T^3 and Y couplings. Furthermore, $SU(2)_L$ invariance requires $Y_L^i = Y_R^i = Y$ for the $SU(2)_L$ component fields. The W^1 interactions to new fermions are given by

$$\mathcal{L} \supset \frac{g}{2} W_\mu^1 (\bar{\mathcal{X}}_{1L} \gamma^\mu \mathcal{X}_{2L} + \bar{\mathcal{X}}_{1R} \gamma^\mu \mathcal{X}_{2R}) + h.c. . \quad (3)$$

At this level, the \mathcal{X}_1 and \mathcal{X}_2 are degenerate owing to the $SU(2)_L$ symmetry. By introducing Yukawa couplings to the SM Higgs, this degeneracy can be broken. In order to write down Yukawa couplings with the SM Higgs and the \mathcal{X} , we can introduce two $SU(2)_L$ singlet vector-like fermions $\xi = (1, Y_\chi + 1/2)$ and $\Upsilon = (1, Y_\chi - 1/2)$, written as Dirac fermions.

In this case we can write the Yukawa couplings

$$\mathcal{L}_{\text{Yuk}} \supset -\lambda_\xi \bar{\mathcal{X}} \cdot H^* \xi - \lambda_\Upsilon \bar{\mathcal{X}} H \Upsilon + h.c. , \quad (4)$$

where the “dot” represents the antisymmetric product. EWSB will then mix these new fermions and will split the \mathcal{X}_1 and \mathcal{X}_2 masses. The sign of λ is not physical, since in the change $\lambda_{\xi, \Upsilon} \rightarrow -\lambda_{\xi, \Upsilon}$, the sign can be absorbed away by a redefinition $\xi \rightarrow -\xi$ and $\Upsilon \rightarrow -\Upsilon$ without affecting anything else.

The only gauge interactions that the vector-like singlets have is the hypercharge B_μ interactions given by

$$\mathcal{L} \supset \sum_i g' B_\mu [\bar{\xi} \gamma^\mu Y_\xi \xi + \bar{\Upsilon} \gamma^\mu Y_\Upsilon \Upsilon] . \quad (5)$$

Next we comment on possible mixing terms for the SM hypercharge assignments $Y_\chi = 1/6$ or $Y_\chi = -1/2$. With only the \mathcal{X} added without the Υ and ξ , for the SM Y_χ assignment $Y_\chi = 1/6$, we can write the additional terms

$$\mathcal{L} \supset -M_{q\chi}\bar{q}\mathcal{X} - \lambda'_u\bar{\mathcal{X}} \cdot H^*u_R - \lambda'_d\bar{\mathcal{X}}Hd_R + h.c. , \quad (6)$$

where q is the SM quark doublet, and u_R, d_R are SM SU(2) singlets. Alternately, if $Y_\chi = -1/2$, then we can write the additional terms

$$\mathcal{L} \supset -M_{\ell\chi}\bar{\ell}\mathcal{X} - \lambda'_\nu\bar{\mathcal{X}} \cdot H^*\nu_R - \lambda'_e\bar{\mathcal{X}}He_R + h.c. , \quad (7)$$

where ℓ is the SM lepton doublet, and ν_R, e_R are SM SU(2) singlets. After EWSB the Yukawa couplings will split the \mathcal{X}_1 and \mathcal{X}_2 masses, and will also mix the new vector-like fermions with either the u_L and d_L in the first case, or with ν_L and e_L in the latter case. In addition to the \mathcal{X} , with the ξ, Υ also added, for $Y_\chi = 1/6$, we can also write the terms

$$\mathcal{L} \supset -M_{u\xi}\bar{u}_R\xi - M_{d\Upsilon}\bar{d}_R\Upsilon - \lambda'_{q\xi}\bar{q} \cdot H^*\xi - \lambda'_{q\Upsilon}\bar{q}H\Upsilon + h.c. . \quad (8)$$

Alternately, if $Y_\chi = -1/2$, then we can also write the terms

$$\mathcal{L} \supset -M_{\nu\xi}\bar{\nu}_R\xi - M_{e\Upsilon}\bar{e}_R\Upsilon - \lambda'_{\ell\xi}\bar{\ell} \cdot H^*\xi - \lambda'_{\ell\Upsilon}\bar{\ell}H\Upsilon + h.c. . \quad (9)$$

Above, the M and λ' are 3×3 Hermitian matrices but the generation indices have been suppressed. If lepton-number is not a good symmetry, and if ξ is a gauge singlet, one can in addition write a Majorana mass term¹

$$\mathcal{L} \supset -\bar{M}_\xi\bar{\xi}^c\xi - (\bar{M}_{\nu\xi}\bar{\nu}_R^c\xi + h.c.) , \quad (10)$$

where ξ^c is the charge conjugated field of the 4-component spinor ξ , and similarly for ν_R^c .

With the mixing M and λ' terms added, there is no longer freedom to rotate away the sign of the λ, λ' , and therefore the sign becomes physical. Since in this work, to be safe from flavor constraints, we take the $M_{SM-VL} \ll M_{VL}$, and $\lambda' \ll 1$, these physical effects will be suppressed, and we therefore do not investigate it further.² We will comment further about these possibilities later.

\mathcal{X}^c equivalence: Since we are dealing with a vector-like theory, it should not matter whether we write the theory in terms of \mathcal{X} with hypercharge Y_χ or in terms of $\mathcal{X}^c \equiv -i\gamma^2\mathcal{X}^*$ with hypercharge $-Y_\chi$. To show this, let us rewrite the theory in terms of \mathcal{X}^c . To relate conjugated and unconjugated terms, we use the relations $\bar{\Psi}^c\mathcal{X}^c = \bar{\mathcal{X}}\Psi$, $\bar{\Psi}^c\gamma^\mu\mathcal{X}^c = -\bar{\mathcal{X}}\gamma^\mu\Psi$. Using these identities we can write the Yukawa term either as $\lambda_\Upsilon\bar{\mathcal{X}}H\Upsilon$ or as $\lambda_\Upsilon\bar{\Upsilon}^cH^T\mathcal{X}^c$. The mass terms, their diagonalization, mass eigenvalues are all identical whether written in terms of \mathcal{X} or \mathcal{X}^c . The gauge interactions on the other hand are opposite in sign, which we understand to mean that the conjugated fields have opposite ‘‘charge’’.

In the theoretical structure just described, we consider in the next few subsections various models.

¹We thank Pedro Schwaller for reminding us of this possibility.

² Refs. [46, 47] consider models with mixing terms present in the context of the muon ($g-2$). Ref. [48] obtains the FCNC constraints due to mixing with a down-type singlet vector-like quark.

2.1 The $1\bar{1}$ Model

For SM-like hypercharge assignments, these vector-like $SU(2)$ singlets can mix with the SM $SU(2)$ singlets and will alter Higgs, electroweak, and flavor observables. If such mixing is sizable, the constraints from flavor observables can be rather strong, due to which we will not consider this possibility here. Ref. [49] discusses the Higgs phenomenology of vector-like leptons with mixing to SM singlets.

For non-SM-like hypercharge assignments with vector-like pairs of $SU(2)$ singlet fermions added, no new (renormalizable) interactions involving the Higgs field can be written down. Thus, there is no modification to Higgs observables, to electroweak precision, or to flavor observables. This will therefore be uninteresting in the present context.

2.2 The $2\bar{2}$ Model

For SM Y_χ assignments, as mentioned earlier, Yukawa couplings can be written down between the χ and the SM right-handed singlets. We do not analyze in much detail the situation when sizable Yukawa couplings with SM $SU(2)$ singlets are allowed as constraints on this (for example, coming from shifts in $Zb\bar{b}$ coupling, FCNC, etc.) are quite severe. This is discussed for instance in Ref. [36], where it is argued that after imposing constraints, the deviation from the SM case of the Higgs observables are at most a few percent.

For non-SM-like hypercharge assignments, with only a vector-like pair of $SU(2)$ -doublets added in with no singlets, no new (renormalizable) interactions can be written down involving the Higgs field. Such an extension will therefore not lead to any new contributions to Higgs boson phenomenology that are significant. So this will be uninteresting in the present context, and we will move to discussing in the following subsections, models with one or more singlets added.

2.3 The $2\bar{2}(1\bar{1})_1$ Model

To understand the nature of this model, we consider in turn the model with only one singlet field present at a time in addition to the \mathcal{X} , namely, first with only the Υ present and then with only the ξ .

2.3.1 Υ Model

In addition to the $SU(2)_L$ multiplet \mathcal{X} , let's consider only one vector-like $SU(2)$ singlet pair in the theory, namely the Υ (without the ξ) with only the λ_Υ term present in Eq. (4). This, as we will see, is sufficient to split the \mathcal{X}_1 and \mathcal{X}_2 masses. Since $Y_H = 1/2$ as usual, for $U(1)_Y$ invariance we need

$$Y_\Upsilon = Y_\chi - 1/2 .$$

Consistent with all the SM gauge symmetries we can write a vector-like mass term as shown in Eq. (1), which is

$$\mathcal{L} \supset -M_\chi \bar{\mathcal{X}} \mathcal{X} = -M_\chi (\bar{\mathcal{X}}_1 \mathcal{X}_1 + \bar{\mathcal{X}}_2 \mathcal{X}_2) . \quad (11)$$

After EWSB by $\langle H \rangle = (0 \ v)^T / \sqrt{2}$, we have the mass matrix

$$\mathcal{L}_{\text{mass}} \supset -M_\chi \bar{\mathcal{X}}_1 \mathcal{X}_1 - (\bar{\mathcal{X}}_2 \ \bar{\Upsilon}) \begin{pmatrix} M_\chi & m \\ m & M_\Upsilon \end{pmatrix} \begin{pmatrix} \mathcal{X}_2 \\ \Upsilon \end{pmatrix} , \quad (12)$$

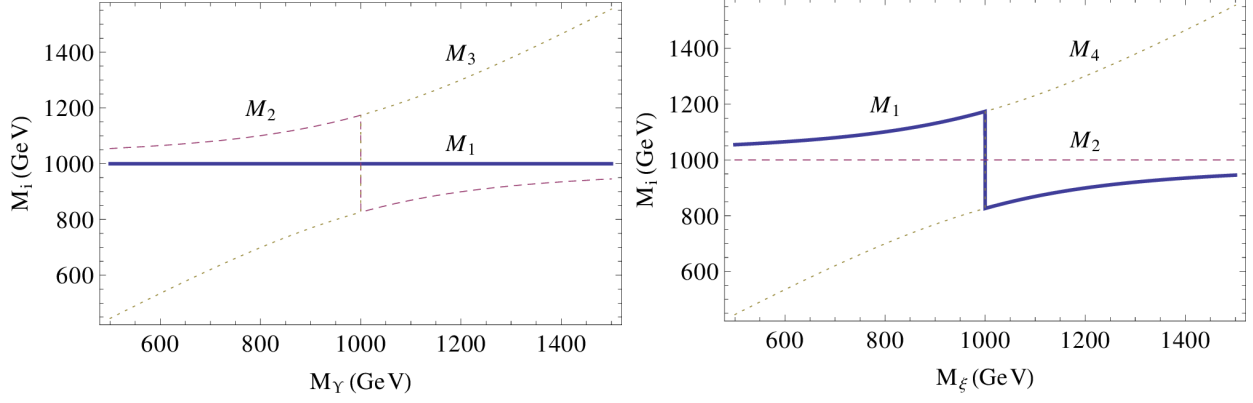


Figure 1: The mass eigenvalues m_i as a function of the SU(2) singlet mass taking the SU(2) doublet mass $M_\chi = 1000$ GeV, and $\lambda_{\Upsilon,\xi} = 1$, in the Υ model (left) and ξ model (right).

where $m \equiv \lambda_\Upsilon v / \sqrt{2}$, which we will assume to be real for simplicity. The above mass matrix is diagonalized by an $O(2)$ rotation

$$\begin{pmatrix} \mathcal{X}_2 \\ \Upsilon \end{pmatrix} = \begin{pmatrix} c_V & -s_V \\ s_V & c_V \end{pmatrix} \begin{pmatrix} \mathcal{X}'_2 \\ \mathcal{X}'_3 \end{pmatrix}, \quad (13)$$

where $\{\mathcal{X}'_i\}$ denote the mass eigenstates, and, $c_V \equiv \cos \theta_V$, $s_V \equiv \sin \theta_V$, with the mixing angle given by

$$\tan 2\theta_V = \frac{2m}{(M_\chi - M_\Upsilon)}. \quad (14)$$

The mass eigenvalues M_i are

$$M_1 = M_\chi; \quad M_{2,3} = \frac{1}{2} \left[M_\chi + M_\Upsilon \pm \sqrt{(M_\chi - M_\Upsilon)^2 + 4m^2} \right], \quad (15)$$

which can also be written as

$$M_1 = M_\chi; \quad M_2 = M_\chi c_V^2 + M_\Upsilon s_V^2 + 2ms_V c_V; \quad M_3 = M_\chi s_V^2 + M_\Upsilon c_V^2 - 2ms_V c_V. \quad (16)$$

To have non-negative M_2 one requires $M_\chi M_\Upsilon - m^2 \geq 0$. In Fig. 1 we show the mass eigenvalues M_i as a function of M_Υ taking $M_\chi = 1000$ GeV and $\lambda_\Upsilon = 1$. Henceforth we drop the primes on the mass eigenstate fields for notational ease. Taking the EM charges of the mass eigenstates \mathcal{X}_i as Q_i , we have, $Q_1 = Y_\chi + 1/2$, $Q_2 = Q_3 = Y_\chi - 1/2$. We show in Table 1 the Q_i for various choices of Y_χ in the Υ model, and Q_4 should be ignored for this model.

The W_μ^1 , W_μ^3 and B_μ interaction terms in Eqs. (2), (3) and (5) in the fermion mass basis become

$$\begin{aligned} \mathcal{L} \supset & + \frac{g}{2} W_\mu^3 [\bar{\mathcal{X}}_1 \gamma^\mu \mathcal{X}_1 - (c_V^2 \bar{\mathcal{X}}_2 \gamma^\mu \mathcal{X}_2 - c_V s_V \bar{\mathcal{X}}_2 \gamma^\mu \mathcal{X}_3 - c_V s_V \bar{\mathcal{X}}_3 \gamma^\mu \mathcal{X}_2 + s_V^2 \bar{\mathcal{X}}_3 \gamma^\mu \mathcal{X}_3)] \\ & + \frac{g}{2} W_\mu^1 [c_V \bar{\mathcal{X}}_2 \gamma^\mu \mathcal{X}_1 - s_V \bar{\mathcal{X}}_3 \gamma^\mu \mathcal{X}_1 + c_V \bar{\mathcal{X}}_1 \gamma^\mu \mathcal{X}_2 - s_V \bar{\mathcal{X}}_1 \gamma^\mu \mathcal{X}_3] \\ & + g' B_\mu [Y_\chi \bar{\mathcal{X}}_1 \gamma^\mu \mathcal{X}_1 + (Y_\chi c_V^2 + Y_\Upsilon s_V^2) \bar{\mathcal{X}}_2 \gamma^\mu \mathcal{X}_2 \\ & \quad + (-Y_\chi + Y_\Upsilon) s_V c_V (\bar{\mathcal{X}}_2 \gamma^\mu \mathcal{X}_3 + h.c.) + (Y_\chi s_V^2 + Y_\Upsilon c_V^2) \bar{\mathcal{X}}_3 \gamma^\mu \mathcal{X}_3]. \end{aligned} \quad (17)$$

Writing this in the A, Z basis we have

$$\begin{aligned} \mathcal{L} \supset & e [\bar{\mathcal{X}}_1 Q_1 \gamma^\mu \mathcal{X}_1 + \bar{\mathcal{X}}_2 Q_2 \gamma^\mu \mathcal{X}_2 + \bar{\mathcal{X}}_3 Q_3 \gamma^\mu \mathcal{X}_3] A_\mu \\ & + g_Z \left[\bar{\mathcal{X}}_1 \left(\frac{1}{2} - s_W^2 Q_1 \right) \gamma^\mu \mathcal{X}_1 + \bar{\mathcal{X}}_2 \left(-\frac{c_V^2}{2} - s_W^2 Q_2 \right) \gamma^\mu \mathcal{X}_2 \right. \\ & \left. + \bar{\mathcal{X}}_3 \left(-\frac{s_V^2}{2} - s_W^2 Q_3 \right) \gamma^\mu \mathcal{X}_3 + \left(\bar{\mathcal{X}}_2 \frac{s_V c_V}{2} \mathcal{X}_3 + \text{h.c.} \right) \right] Z_\mu, \end{aligned} \quad (18)$$

where $g_Z = g/c_W$, $Q_1 \equiv 1/2 + Y_\mathcal{X}$ and $Q_2 = Q_3 = -1/2 + Y_\mathcal{X} = Y_\Upsilon$.

The Higgs interactions are got by replacing $v \rightarrow v(1 + h/v)$ in Eq. (12). In the mass basis this gives

$$\mathcal{L} \supset -\frac{\lambda_\Upsilon}{\sqrt{2}} h [s_V c_V \bar{\mathcal{X}}_2 \mathcal{X}_2 - s_V c_V \bar{\mathcal{X}}_3 \mathcal{X}_3 + (c_V^2 - s_V^2) \bar{\mathcal{X}}_3 \mathcal{X}_2] + \text{h.c.} . \quad (19)$$

We commented below Eqs. (4) and (9) that the sign of the Yukawa couplings can be absorbed away by redefining the fields if the Yukawa terms mixing the \mathcal{X} and SM fermions are taken negligibly small. They are therefore not physical in the limit of the mixing Yukawa couplings not present. For later use we note in this model that under $\lambda_\Upsilon \rightarrow -\lambda_\Upsilon$, we have $m \rightarrow -m$, $\theta_V \rightarrow -\theta_V$, $s_V \rightarrow -s_V$. Therefore, off-diagonal (in fermion fields) couplings of the h and Z_μ change sign (i.e. the $h\mathcal{X}_3\mathcal{X}_2$ and $Z\mathcal{X}_3\mathcal{X}_2$ couplings), while all the diagonal couplings do not change sign.

2.3.2 ξ Model

In addition to the $SU(2)_L$ multiplet \mathcal{X} , lets consider only one vector-like $SU(2)$ singlet pair in the theory, namely the ξ (without the Υ) with only the λ_ξ term present in Eq. (4). Since $Y_H = 1/2$ as usual, for $U(1)_Y$ invariance we need

$$Y_\xi = Y_\mathcal{X} + 1/2 .$$

After EWSB by $\langle H \rangle = (0 \ v)^T/\sqrt{2}$, we have the mass matrix

$$\mathcal{L}_{\text{mass}} \supset -M_\mathcal{X} \bar{\mathcal{X}}_2 \mathcal{X}_2 - \begin{pmatrix} \bar{\mathcal{X}}_1 & \bar{\xi} \end{pmatrix} \begin{pmatrix} M_\mathcal{X} & \tilde{m} \\ \tilde{m} & M_\xi \end{pmatrix} \begin{pmatrix} \mathcal{X}_1 \\ \xi \end{pmatrix}, \quad (20)$$

where $\tilde{m} \equiv \lambda_\xi v/\sqrt{2}$, which we will assume to be real for simplicity. The above mass matrix is diagonalized by an $O(2)$ rotation

$$\begin{pmatrix} \mathcal{X}_1 \\ \xi \end{pmatrix} = \begin{pmatrix} c'_V & -s'_V \\ s'_V & c'_V \end{pmatrix} \begin{pmatrix} \mathcal{X}'_1 \\ \mathcal{X}'_4 \end{pmatrix}, \quad (21)$$

where $\{\mathcal{X}'_i\}$ denote the mass eigenstates, and, $c'_V \equiv \cos \theta'_V$, $s'_V \equiv \sin \theta'_V$, with the mixing angle given by

$$\tan 2\theta'_V = \frac{2\tilde{m}}{(M_\mathcal{X} - M_\xi)}. \quad (22)$$

The mass eigenvalues M_i are

$$M_2 = M_\mathcal{X}; \quad M_{1,4} = \frac{1}{2} \left[M_\mathcal{X} + M_\xi \pm \sqrt{(M_\mathcal{X} - M_\xi)^2 + 4\tilde{m}^2} \right], \quad (23)$$

which can also be written as

$$M_2 = M_\mathcal{X}; \quad M_1 = M_\mathcal{X} c_V'^2 + M_\xi s_V'^2 + 2\tilde{m} s'_V c'_V; \quad M_4 = M_\mathcal{X} s_V'^2 + M_\xi c_V'^2 - 2\tilde{m} s'_V c'_V. \quad (24)$$

To have non-negative M_1 one requires $M_\chi M_\xi - \tilde{m}^2 \geq 0$. Henceforth we drop the primes on the mass eigenstate fields for notational ease. Taking the EM charges of the mass eigenstates \mathcal{X}_i as Q_i , we have, $Q_2 = Y_\chi - 1/2$, $Q_1 = Q_4 = Y_\chi + 1/2$. We show in Table 1 the Q_i for various choices of Y_χ in the ξ model, and Q_3 should be ignored for this model.

The W_μ^1 , W_μ^3 and B_μ interaction terms in Eqs. (2), (3) and (5) in the fermion mass basis become

$$\begin{aligned} \mathcal{L} \supset & + \frac{g}{2} W_\mu^3 [c_V'^2 \bar{\mathcal{X}}_1 \gamma^\mu \mathcal{X}_1 - c_V' s_V' \bar{\mathcal{X}}_1 \gamma^\mu \mathcal{X}_4 - c_V' s_V' \bar{\mathcal{X}}_4 \gamma^\mu \mathcal{X}_1 + s_V'^2 \bar{\mathcal{X}}_4 \gamma^\mu \mathcal{X}_4 - \bar{\mathcal{X}}_2 \gamma^\mu \mathcal{X}_2] \\ & + \frac{g}{2} W_\mu^1 [c_V' \bar{\mathcal{X}}_2 \gamma^\mu \mathcal{X}_1 - s_V' \bar{\mathcal{X}}_2 \gamma^\mu \mathcal{X}_4 + h.c.] \\ & + g' B_\mu [(Y_\chi c_V'^2 + Y_\xi s_V'^2) \bar{\mathcal{X}}_1 \gamma^\mu \mathcal{X}_1 + (-Y_\chi + Y_\xi) s_V' c_V' (\bar{\mathcal{X}}_1 \gamma^\mu \mathcal{X}_4 + h.c.) \\ & \quad + (Y_\chi s_V'^2 + Y_\xi c_V'^2) \bar{\mathcal{X}}_4 \gamma^\mu \mathcal{X}_4 + Y_\chi \bar{\mathcal{X}}_2 \gamma^\mu \mathcal{X}_2] . \end{aligned} \quad (25)$$

The Higgs interactions are got by replacing $v \rightarrow v(1 + h/v)$ in Eq. (12). In the mass basis this gives

$$\mathcal{L} \supset -\frac{\lambda_\xi}{\sqrt{2}} h [s_V' c_V' \bar{\mathcal{X}}_1 \mathcal{X}_1 - s_V' c_V' \bar{\mathcal{X}}_4 \mathcal{X}_4 + (c_V'^2 - s_V'^2) \bar{\mathcal{X}}_4 \mathcal{X}_1] + h.c. . \quad (26)$$

2.3.3 Alternate Yukawa coupling

Instead of the Yukawa coupling of the Υ shown in Eq. (4) we can alternately write

$$\mathcal{L}_{\text{Yuk Alt}} \supset \hat{\lambda}_\Upsilon \bar{\mathcal{X}}^c H \Upsilon + h.c. , \quad (27)$$

where we use the fact that $i\sigma^2 \mathcal{X}^*$ transforms the same way as \mathcal{X} under $SU(2)$ and have defined $\bar{\mathcal{X}}^c$ to mean this conjugation in gauge space and also conjugation in spinor space. In this case we have for $U(1)_Y$ invariance, $\hat{Y}_\Upsilon = -Y_\chi - 1/2$. While we can write a similar alternate coupling for the ξ also, we do not explicitly write it here. With the alternate Yukawa coupling Eq. (27) in the Υ model, the mass terms are

$$\mathcal{L}_{\text{mass}}^\Upsilon \supset -M_\chi \bar{\mathcal{X}}_2^c \mathcal{X}_2^c - (\bar{\mathcal{X}}_1^c \quad \bar{\Upsilon}) \begin{pmatrix} M_\chi & \hat{m} \\ \hat{m} & M_\Upsilon \end{pmatrix} \begin{pmatrix} \mathcal{X}_1^c \\ \Upsilon \end{pmatrix} , \quad (28)$$

where $\hat{m} \equiv \hat{\lambda}_\Upsilon v / \sqrt{2}$. This mass matrix is identical to that in the theory with the ξ model shown in Eq. (20), but now written for $(\mathcal{X}_1^c, \mathcal{X}_2^c)$ instead of $(\mathcal{X}_1, \mathcal{X}_2)$. So the mass eigenvalues are the same as in the ξ model. Furthermore, due to the conjugation, all the gauge couplings are with opposite sign to what is in the model with only the ξ .

2.4 The $2\bar{2}(1\bar{1})_2$ Model

Here we consider the addition of both the $SU(2)$ singlet fields Υ and ξ , in addition to the $SU(2)_L$ doublet field \mathcal{X} , and turning on both Yukawa couplings in Eq. (4), namely λ_Υ and λ_ξ . For $U(1)_Y$ invariance, we recall that Υ has hypercharge $Y_\chi - 1/2$ and ξ has hypercharge $Y_\chi + 1/2$.

After EWSB, Eq. (4) will generate mass mixing terms

$$\mathcal{L}_{\text{mass}} \supset -(\bar{\mathcal{X}}_1 \quad \bar{\xi}) \begin{pmatrix} M_\chi & \tilde{m} \\ \tilde{m} & M_\xi \end{pmatrix} \begin{pmatrix} \mathcal{X}_1 \\ \xi \end{pmatrix} - (\bar{\mathcal{X}}_2 \quad \bar{\Upsilon}) \begin{pmatrix} M_\chi & m \\ m & M_\Upsilon \end{pmatrix} \begin{pmatrix} \mathcal{X}_2 \\ \Upsilon \end{pmatrix} , \quad (29)$$

where $m \equiv \lambda_\Upsilon v / \sqrt{2}$ and $\tilde{m} \equiv \lambda_\xi v / \sqrt{2}$, both of which we will assume to be real for simplicity. The above mass matrix is diagonalized by two $O(2)$ rotations

$$\begin{pmatrix} \mathcal{X}_1 \\ \xi \end{pmatrix} = \begin{pmatrix} c_V' & -s_V' \\ s_V' & c_V' \end{pmatrix} \begin{pmatrix} \mathcal{X}'_1 \\ \xi' \end{pmatrix} ; \quad \begin{pmatrix} \mathcal{X}_2 \\ \Upsilon \end{pmatrix} = \begin{pmatrix} c_V & -s_V \\ s_V & c_V \end{pmatrix} \begin{pmatrix} \mathcal{X}'_2 \\ \Upsilon' \end{pmatrix} , \quad (30)$$

Table 1: Q_i for various choices of $Y_\chi = \pm Y_{SM}$. Q_4 should be ignored in the $2\bar{2}(1\bar{1})_1$ Υ model, Q_3 should be ignored in $2\bar{2}(1\bar{1})_1$ ξ model, and all four states are present in the $2\bar{2}(1\bar{1})_2$ model.

Y_χ	-1/2	-1/6	1/6	1/2
Q_1, Q_4	0	1/3	2/3	1
Q_2, Q_3	-1	-2/3	-1/3	0

where $\{\mathcal{X}'_i\}$ denote the mass eigenstates, and, $c_V \equiv \cos \theta_V$, $s_V \equiv \sin \theta_V$, with the mixing angle given by

$$\tan 2\theta'_V = \frac{2\tilde{m}}{(M_\chi - M_\xi)} ; \quad \tan 2\theta_V = \frac{2m}{(M_\chi - M_\Upsilon)} . \quad (31)$$

The mass eigenvalues M_i are

$$\begin{aligned} M_{1,4} &= \frac{1}{2} \left[M_\chi + M_\xi \pm \sqrt{(M_\chi - M_\xi)^2 + 4\tilde{m}^2} \right] ; \\ M_{2,3} &= \frac{1}{2} \left[M_\chi + M_\Upsilon \pm \sqrt{(M_\chi - M_\Upsilon)^2 + 4m^2} \right] , \end{aligned} \quad (32)$$

which can also be written as

$$\begin{aligned} M_1 &= M_\chi c_V'^2 + M_\xi s_V'^2 + 2\tilde{m}s_V'c_V' ; & M_4 &= M_\chi s_V'^2 + M_\xi c_V'^2 - 2\tilde{m}s_V'c_V' ; \\ M_2 &= M_\chi c_V^2 + M_\Upsilon s_V^2 + 2ms_Vc_V ; & M_3 &= M_\chi s_V^2 + M_\Upsilon c_V^2 - 2ms_Vc_V . \end{aligned} \quad (33)$$

To have non-negative M_1 and M_2 one requires $M_\chi M_\Upsilon - m^2 \geq 0$ and $M_\chi M_\xi - \tilde{m}^2 \geq 0$ respectively. Henceforth we drop the primes on the mass eigenstate fields for notational ease. Taking the EM charges of the mass eigenstates \mathcal{X}_i as Q_i , we have, $Q_1 = Q_4 = Y_\chi + 1/2$, $Q_2 = Q_3 = Y_\chi - 1/2$. We show in Table 1 the Q_i for various choices of Y_χ .

The W_μ^1, W_μ^3 and B_μ interaction terms in Eqs. (2), (3) and (5) in the fermion mass basis become

$$\begin{aligned} \mathcal{L} \supset & + \frac{g}{2} W_\mu^3 \left[(c_V'^2 \bar{\mathcal{X}}_1 \gamma^\mu \mathcal{X}_1 - c_V' s_V' \bar{\mathcal{X}}_1 \gamma^\mu \mathcal{X}_4 - c_V' s_V' \bar{\mathcal{X}}_4 \gamma^\mu \mathcal{X}_1 + s_V'^2 \bar{\mathcal{X}}_4 \gamma^\mu \mathcal{X}_4) \right. \\ & \left. - (c_V^2 \bar{\mathcal{X}}_2 \gamma^\mu \mathcal{X}_2 - c_V s_V \bar{\mathcal{X}}_2 \gamma^\mu \mathcal{X}_3 - c_V s_V \bar{\mathcal{X}}_3 \gamma^\mu \mathcal{X}_2 + s_V^2 \bar{\mathcal{X}}_3 \gamma^\mu \mathcal{X}_3) \right] \\ & + \frac{g}{2} W_\mu^1 \left[c_V c_V' \bar{\mathcal{X}}_2 \gamma^\mu \mathcal{X}_1 - c_V s_V' \bar{\mathcal{X}}_2 \gamma^\mu \mathcal{X}_4 - s_V c_V' \bar{\mathcal{X}}_3 \gamma^\mu \mathcal{X}_1 + s_V s_V' \bar{\mathcal{X}}_3 \gamma^\mu \mathcal{X}_4 + h.c. \right] \\ & + g' B_\mu \left[(Y_\chi c_V'^2 + Y_\xi s_V'^2) \bar{\mathcal{X}}_1 \gamma^\mu \mathcal{X}_1 + (-Y_\chi + Y_\xi) s_V' c_V' (\bar{\mathcal{X}}_1 \gamma^\mu \mathcal{X}_4 + h.c.) + (Y_\chi s_V'^2 + Y_\xi c_V'^2) \bar{\mathcal{X}}_4 \gamma^\mu \mathcal{X}_4 \right. \\ & \left. + (Y_\chi c_V^2 + Y_\Upsilon s_V^2) \bar{\mathcal{X}}_2 \gamma^\mu \mathcal{X}_2 + (-Y_\chi + Y_\Upsilon) s_V c_V (\bar{\mathcal{X}}_2 \gamma^\mu \mathcal{X}_3 + h.c.) + (Y_\chi s_V^2 + Y_\Upsilon c_V^2) \bar{\mathcal{X}}_3 \gamma^\mu \mathcal{X}_3 \right] . \end{aligned} \quad (34)$$

The Higgs interactions are got by replacing $v \rightarrow v(1 + h/v)$ in Eq. (12), which in the fermion mass basis is

$$\begin{aligned} \mathcal{L} \supset & \left\{ -\frac{\lambda_\xi}{\sqrt{2}} h \left[s_V' c_V' \bar{\mathcal{X}}_1 \mathcal{X}_1 - s_V' c_V' \bar{\mathcal{X}}_4 \mathcal{X}_4 + (c_V'^2 - s_V'^2) \bar{\mathcal{X}}_4 \mathcal{X}_1 \right] \right. \\ & \left. - \frac{\lambda_\Upsilon}{\sqrt{2}} h \left[s_V c_V \bar{\mathcal{X}}_2 \mathcal{X}_2 - s_V c_V \bar{\mathcal{X}}_3 \mathcal{X}_3 + (c_V^2 - s_V^2) \bar{\mathcal{X}}_3 \mathcal{X}_2 \right] \right\} + h.c. . \end{aligned} \quad (35)$$

2.5 Some vector-like Extensions of the SM

We add to the SM some number of vector-like colored (quark) and uncolored (lepton) doublets and singlets corresponding to the $2\bar{2}(1\bar{1})_1$ or $2\bar{2}(1\bar{1})_2$ framework outlined in the previous subsection. For

notational ease, we refer to the quark $SU(2)$ doublet \mathcal{X}_Q simply as Q , quark $SU(2)$ singlets ξ_U as U and Υ_D as D , and, the lepton $SU(2)$ doublet \mathcal{X}_L as L , $SU(2)$ singlets Υ_E as E and ξ_N as N . From the context it should be clear that we are referring to the new vector-like fermions and not the SM ones. These vector-like quarks and leptons have EM charges same as the corresponding SM quarks and leptons only for the specific hypercharge Y_χ assignments of $Y_Q = 1/6$ and $Y_L = -1/2$ respectively. We give below the nomenclature of the models with the addition of various vector-like $SU(2)$ doublet and singlet quarks and leptons to the SM:

- Minimal vector-like Quark: The $2\bar{2}(1\bar{1})_1$ model in the $SU(3)_c$ fundamental representation, with an $SU(2)$ doublet quark \mathcal{X}_Q and *one* $SU(2)$ singlet quark; with only the Υ_D will be the $MVQD_1$, while with only the ξ_U will be the $MVQU_1$. n copies of these will be called $MVQD_n$ and $MVQU_n$.
- vector-like quark (VQ): The $2\bar{2}(1\bar{1})_2$ model in the $SU(3)_c$ fundamental representation, with an $SU(2)$ doublet quark \mathcal{X}_Q and two $SU(2)$ singlet quarks Υ_D and ξ_U . n copies of these will be called VQ_n .
- Minimal vector-like lepton: The $2\bar{2}(1\bar{1})_1$ model which is an $SU(3)_c$ singlet, with an $SU(2)$ doublet lepton \mathcal{X}_L and *one* $SU(2)$ singlet lepton; with only the Υ_E will be the $MVLE_1$, while with only the ξ_N will be the $MVLN_1$. n copies of these will be called $MVLE_n$ and $MVLN_n$.
- vector-like lepton (VL): The $2\bar{2}(1\bar{1})_2$ model which is an $SU(3)_c$ singlet, with an $SU(2)$ doublet lepton \mathcal{X}_L and two $SU(2)$ singlet leptons Υ_E and ξ_N . n copies of these will be called VL_n .
- The minimal vector-like extension of the SM (MVSM): $MVQ\{D,U\} + MVL\{E,N\}$ forms the 1-generation $MVSM_{\{D,U,E,N\}}$. n copies of these will form the n-generation MVSM.
- The vector-like extension of the SM (VSM): $VQ + VL$ forms the 1-generation VSM (VSM_1). n copies of these will form the n-generation VSM, called here VSM_n .

For some Y_Q and Y_L assignments and in some region of parameter-space it is possible that the lightest vector-like particle is uncolored and EM neutral. Such a state, if stable, can be a possible dark matter candidate. For example, in the $MVLE$ model with $Y_L = 1/2$ there are two EM neutral uncolored states, and if stable, the lighter of these can be a dark matter candidate. Alternately, if the lightest vector-like particle is colored and stable, is it possible that a color-singlet bound-state of this (either with another vector-like particle or with an SM quark) could be the dark matter? A detailed investigation of this possibility is beyond the scope of this work, but such a strongly interacting dark matter (SIMP) candidate appears to be heavily disfavored as discussed for example in Refs. [50, 51, 52, 53, 54, 55].

The addition of vector-like fermions changes the running of the Higgs quartic coupling and the vacuum can become unstable at some energy scale Λ . We will treat the theory we have written down as an effective theory valid below the scale Λ . Refs. [31, 34] derive the vacuum stability constraint with vector-like leptons only, in a model similar to our VL_n . Ref. [34] finds, for example for $\lambda = 1$, that $\Lambda \approx 2.5$ TeV for the lightest charged lepton mass of 100 GeV. For vector-like lepton masses of 200, 450 GeV (for the two mass eigenstates), Ref. [31] finds $\Lambda \sim 10$ TeV. Since their main motivation is obtaining a large $\mu_{\gamma\gamma} \approx (1.5, 2)$, they need large Yukawa couplings for large vector-like masses, and therefore one would expect stronger constraints in their case than in ours. Ref. [56] analyzes the vacuum stability issue when new physics contribution changes the sign of the ggh and $\gamma\gamma h$ effective vertices (while keeping the magnitude the same as in the SM). Ref. [57] works out the vacuum stability constraints in the case when the vector-like fermion mass is tied to the scale

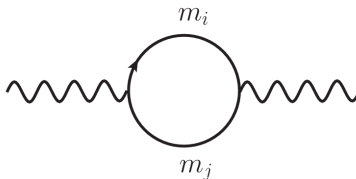


Figure 2: The vector-like fermion contribution to the gauge 2-point function $\Pi^{(m_i m_j)}$.

of EWSB. Ref. [58] considers the possibility of a strongly first-order electroweak phase transition driven by heavy vector-like fermions. Working out the precise value of Λ in our case will be taken up in future work.

We focus here on SM-like $SU(3)$, $SU(2)_L$ and $U(1)_Y$ representations, and a more general analysis with non-SM-like representations will be postponed to future work. Our focus in this work will be the modifications of precision electroweak observables, and, LHC Higgs production and decay, due to the presence of additional vector-like fermions in SM-like representations.

3 Precision Electroweak Observables

One of the great successes of the SM is the near perfect agreement between the indirect constraints on the Higgs mass from precision electroweak observables [59, 60, 61] and the mass of the observed state at the LHC. The precision electroweak constraints have been investigated in the context of a chiral fourth generation elsewhere (see for example Ref. [62] and references therein). In this section, we present the oblique corrections [63, 64, 65] written in terms of the S, T, U parameters [63] due to vector-like fermions. The S, T, U parameters are given by

$$S = -16\pi\Pi'_{3Y}(0) , \quad (36)$$

$$T = \frac{4\pi}{s_W^2 m_W^2} [\Pi_{11}(0) - \Pi_{33}(0)] , \quad (37)$$

$$U = 16\pi [\Pi'_{11}(0) - \Pi'_{33}(0)] . \quad (38)$$

Vector-like quark contributions to S , T and U have been presented earlier in Ref. [66]. Here we derive these including contributions from vector-like quarks and leptons, and in the following sections make contact with properties of the recently observed Higgs boson.

3.1 S, T, U Constraints

The allowed regions in the S and T plane is shown for instance in Refs. [67, 68]. We take the reference Higgs mass and top mass values as $m_h = 125.5$ GeV [69, 70] and $m_t = 173.2$ GeV [71, 72]. We include the ΔS , ΔT and ΔU contributions due to vector-like fermions and ascertain whether they lie within the 68 % or 95 % allowed regions.

The U parameter best-fit value is 0.08 ± 0.11 [67]. Since contributions to U are typically quite small, it does not impose any nontrivial constraints on models. It is therefore acceptable to set U to zero and obtain constraints from S and T ; we adopt this method here.

New vector-like fermions \mathcal{X}^i will generate additional contributions to S , T and U due to the new W^1 , W^3 and B interactions going into the gauge 2-point functions Π shown in Fig. 2. The detailed computation of the Π with vector-like fermions is given in Appendix A. There we define Π_{LL} with a

chirality projector P_L inserted in the first vertex and P_L in the second vertex, and similarly for Π_{RR} , Π_{RL} and Π_{LR} , and, $\Pi \equiv \Pi_{LL} + \Pi_{LR}$, and also, $\Pi^{\{m_i, m_j\}} = \Pi^{(m_i m_j)} + \Pi^{(m_j m_i)}$, $\Pi^{(m_i)} = \Pi^{(m_i m_i)}$. We similarly define Π' . In terms of these Π s computed in Appendix A, we present next the S , T , and U due to vector-like fermions in the $2\bar{2}(1\bar{1})_1$ and $2\bar{2}(1\bar{1})_2$ models of Sections 2.3 and 2.4 respectively.

3.2 S , T , U in the $2\bar{2}(1\bar{1})_1$ model

We work out in turn the S , T , U , first for the model of Sec. 2.3.1 with only the Υ present, and then for the model of Sec. 2.3.2 with only the ξ present.

3.2.1 Υ Model

With only the Υ present, in the $2\bar{2}(1\bar{1})_1$ vector-like model described in Sec. 2.3.1, from the interactions in Eqs. (2), (3) and (5) we compute the gauge boson 2-point functions of Fig. 2 and then S , T and U . We compute $\Pi'_{3\Upsilon}(0)$ and then the S parameter from Eq. (36) as

$$S = -32\pi d_3 \left[T_{11}^3 Y_{\mathcal{X}} \Pi'^{(m_1)}(0) + T_{22}^3 \left(c_V^2 (Y_{\mathcal{X}} c_V^2 + Y_{\Upsilon} s_V^2) \Pi'^{(m_2)}(0) + s_V^2 (Y_{\mathcal{X}} s_V^2 + Y_{\Upsilon} c_V^2) \Pi'^{(m_3)}(0) - c_V^2 s_V^2 (-Y_{\mathcal{X}} + Y_{\Upsilon}) \Pi'^{\{m_2, m_3\}}(0) \right) \right], \quad (39)$$

where d_3 is the dimension of the $SU(3)$ representation of the vector-like fermion (for example, for a fundamental of $SU(3)$, $d_3 = N_c = 3$). The divergent $2/\epsilon$ pieces (along with the $-\gamma + \log 4\pi$ pieces) cancel leaving a finite S . We compute next the T -parameter, for which we compute $\Pi_{11}(0)$ and $\Pi_{33}(0)$ as

$$\Pi_{11} = 2d_3 (T_{12}^1)^2 \left(c_V^2 \Pi^{\{m_1, m_2\}} + s_V^2 \Pi^{\{m_1, m_3\}} \right), \quad (40)$$

$$\Pi_{33} = 2d_3 \left\{ (T_{11}^3)^2 \Pi^{(m_1)} + (T_{22}^3)^2 \left[c_V^4 \Pi^{(m_2)} + s_V^2 c_V^2 \Pi^{\{m_2, m_3\}} + s_V^4 \Pi^{(m_3)} \right] \right\}. \quad (41)$$

T is then given by Eq. (37). Again, the divergent $2/\epsilon$ pieces (along with the $-\gamma + \log 4\pi$ pieces) cancel leaving a finite T . U is computed using Eq. (38) for which the $\Pi'_{11}(0)$ and $\Pi'_{33}(0)$ are got from equations identical to Eqs. (40) and (41) except for replacing $\Pi \rightarrow \Pi'$.

From the \mathcal{X}^c equivalence noted in Sec. 2, we infer that the vector-like fermion contributions to S and T parameters is the same whether written in terms of the \mathcal{X} or \mathcal{X}^c . This is because the 2-point functions shown in Fig. 2 have two gauge interaction vertices although each with opposite sign compared between \mathcal{X} and \mathcal{X}^c formulations, and the loop functions have the same value since the mass eigenvalues are exactly the same in the two formulations.

This is not to say, however, that $Y_{\mathcal{X}}$ and $-Y_{\mathcal{X}}$ should necessarily give the same S , and we do indeed find that S can change sign with the sign of $Y_{\mathcal{X}}$. This is because isospin offers a reference, i.e., in \mathcal{X} , a given isospin component has hypercharge $Y_{\mathcal{X}}$, while in \mathcal{X}^c it has hypercharge $-Y_{\mathcal{X}}$. Furthermore, the Yukawa interaction terms in Eq. (4) couples the vector-like sector to a chiral SM sector, in particular to the Higgs with a specific hypercharge assignment, namely $Y_H = +1/2$. For the two cases with $Y_{\mathcal{X}}$ and $-Y_{\mathcal{X}}$, the $U(1)_Y$ invariance of this Yukawa coupling implies different Υ (or ξ) hypercharges and consequently different electromagnetic charges, and observables can be sensitive to this difference, as for instance the S -parameter.

It is interesting that vector-like fermions can easily give a negative S -parameter. This is unlike in the case of chiral fermions where one finds that the S -parameter is usually positive leading to a tight constraint on dynamical EWSB BSM sectors [63]. Some examples of theories that give a negative S -parameter are also discussed in Refs. [73, 74].

3.2.2 ξ Model

Let us turn to the ξ model described in Sec. 2.3.2. For obtaining the gauge 2-point functions, we notice that we can take the results for the model of Sec. 2.3.1 for the Υ model and interchange $T_{11}^3 \leftrightarrow T_{22}^3$ in the W_μ^3 interactions while keeping W_μ^1 and B_μ interactions the same. This implies that the S -parameter for this model will be the same as that obtained in the model of Sec. 2.3.1 but for *opposite* sign of Y_χ , i.e., $S_{\xi \text{ Model}}(Y_\chi) = S_{\Upsilon \text{ Model}}(-Y_\chi)$. The T -parameter is the same in both the models of Sec. 2.3.1 and Sec. 2.3.2. We have checked that our numerical results are consistent with these expectations.

3.2.3 Υ Model with alternate Yukawa coupling

For the Υ model with the alternate Yukawa coupling of Eq. (27), we noted in Sec. 2.3.3 that the mass matrices are identical to that of the ξ model. Also, the gauge couplings are of opposite sign, but since the vector-like fermion contributions to the gauge 2-point functions have two such couplings, this will not affect the S and T parameters. The last change is the different hypercharge assignment $\tilde{Y}_\Upsilon = -Y_\chi - 1/2$. The S and T parameters for the Υ coupled as in $\mathcal{L}_{\text{Yuk Alt}}$ will in general be different when compared to the Υ model or ξ model. For $Y_\chi = -1/2$, however, we have $\tilde{Y}_\Upsilon = Y_\chi$, and we therefore have

$$S_{\Upsilon \text{ Model}}^{\text{Yuk Alt}}(Y_\chi = -1/2) = S_{\xi \text{ Model}}^{\text{Yuk}}(Y_\chi = -1/2) .$$

3.3 S, T, U in the $2\bar{2}(1\bar{1})_2$ model

In the $2\bar{2}(1\bar{1})_2$ vector-like model described in Sec. 2.4, from the interactions in Eqs. (2), (3) and (5) we can compute the gauge boson 2-point functions of Fig. 2. We find

$$\begin{aligned} \Pi_{11} &= 2d_3(T_{12}^1)^2 \left[c_V^2 c_V'^2 \Pi^{\{M_1, M_2\}} + s_V^2 c_V'^2 \Pi^{\{M_1, M_3\}} + c_V^2 s_V'^2 \Pi^{\{M_2, M_4\}} + s_V^2 s_V'^2 \Pi^{\{M_3, M_4\}} \right] , \\ \Pi_{33} &= 2d_3 \left\{ (T_{11}^3)^2 \left[c_V^4 \Pi^{(M_1)} + s_V'^2 c_V'^2 \Pi^{\{M_1, M_4\}} + s_V^4 \Pi^{(M_4)} \right] \right. \\ &\quad \left. + (T_{22}^3)^2 \left[c_V^4 \Pi^{(M_2)} + s_V^2 c_V^2 \Pi^{\{M_2, M_3\}} + s_V^4 \Pi^{(M_3)} \right] \right\} , \\ \Pi'_{3Y} &= 2d_3 \left\{ (T_{11}^3) \left[c_V'^2 (Y_\chi c_V'^2 + Y_\xi s_V'^2) \Pi'^{(M_1)} - c_V'^2 s_V'^2 (-Y_\chi + Y_\xi) \Pi'^{\{M_1, M_4\}} + s_V'^2 (Y_\chi s_V'^2 + Y_\xi c_V'^2) \Pi'^{(M_4)} \right] \right. \\ &\quad \left. + (T_{22}^3) \left[c_V^2 (Y_\chi c_V^2 + Y_\Upsilon s_V^2) \Pi'^{(M_2)} - c_V^2 s_V^2 (-Y_\chi + Y_\Upsilon) \Pi'^{\{M_2, M_3\}} + s_V^2 (Y_\chi s_V^2 + Y_\Upsilon c_V^2) \Pi'^{(M_3)} \right] \right\} \end{aligned} \quad (42)$$

where the Π and Π' are as given in Eqs. (A.74) and (A.75) respectively. The S, T and U are then given by Eqs. (36), (37) and (38) respectively.

3.4 Shift in the $Zb\bar{b}$ coupling

For $Y_\chi = 1/6, -1/6$ there are vector-like states with EM charge $-1/3$, and if they also have color, these states can mix with the SM b -quark after EWSB. This mixing will imply a shift in the $Zb\bar{b}$ coupling which is constrained by LEP. The measurements $R_b = 0.21629 \pm 0.00066$ and $\Gamma_{hadrons} = 1.7444 \pm 0.0020$ GeV at LEP [67], imply constraints on the $Zb\bar{b}$ coupling. A Yukawa coupling between the SM b and the vector-like b' induces a mixing, which if it's only in the L sector, i.e. between $b_L \leftrightarrow b'_L$ only,³ the $Zb_L\bar{b}_L$ coupling shifts to $-1/2(c_L^2) + (1/3)s_W^2$ where $c_L \equiv \cos\theta_L$ and

³For a concrete example of a theory where this is the case, see Refs. [7, 32].

the mixing angle is given by $\tan(2\theta_L) = (\lambda/\sqrt{2})v/M_{b'}$. This mixing is constrained by the above data and will imply the limit

$$M_{b'}/\lambda \geq 3509 \text{ GeV at } 1\sigma ; \text{ and } M_{b'}/\lambda \geq 2481 \text{ GeV at } 2\sigma . \quad (43)$$

This limit can be evaded by ensuring that the Yukawa couplings between the SM b and b' is not too large, as dictated by Eq. (43). We will assume that this is the case in the rest of our analysis. This limit will be evaded completely in the model where a custodial symmetry protects the $Zb\bar{b}$ coupling (see Ref. [75]). Also, this limit will not be relevant for Y_χ assignments that do not result in a charge $-1/3$ vector-like state.

4 Direct Collider Constraints

4.1 Mass and gauge eigenstates

In order to consider the constraints from colliders, we look at the decays of the vector-like matter. In particular, we are interested in decays via the Higgs and the electroweak gauge bosons. We write the following Lagrangian for the mass sector of the model. We denote the VSM quarks as T_R and B_R , where these are the singlet states under SU(2) that are referred to in previous sections as ξ_U and Υ_D . The states denoted as $T_{\bar{R}}$, $B_{\bar{R}}$ are the left-handed projections of the vector-like singlets. We assume that we are dealing with only one new generation of VSM quarks and leptons, i.e. the VSM₁ in order to get an idea of the constraints. For the sake of simplicity, we do not consider the effects of mixing with the doublet under SU(2), previously denoted as \mathcal{X}_Q , as it will not substantially alter the results. Aside from the assumption that off-diagonal couplings are small relative to the diagonal entries, we do not make any a priori assumptions about their sizes relative to each other, so the mixing between T and the 2nd and 3rd generations can in principle be of similar sizes. Motivated by simplicity and data, we do not consider mixing with the first generation, although this could be implemented, given that the off-diagonal couplings are small. We can write the mass terms as

$$\begin{aligned} \mathcal{L}_{mass} = & m_{cc}\bar{c}_L c_R + m_{ct}\bar{c}_L t_R + m_{cT}\bar{c}_L T_R + m_{tc}\bar{t}_L c_R + m_{tt}\bar{t}_L t_R + m_{tT}\bar{t}_L T_R \\ & + \mu_c \bar{T}_{\bar{R}} c_R + \mu_t \bar{T}_{\bar{R}} t_R + \mu_T \bar{T}_{\bar{R}} T_R \\ & + (c \leftrightarrow s, \quad t \leftrightarrow b, \quad T \leftrightarrow B) , \end{aligned} \quad (44)$$

where m_{ij} is used to denote a mass obtained due to the Higgs VEV in the Yukawa interactions of Sec. 2, and μ_i , which appeared in Sections 2 and 3 as M_ξ , is a vector-like mass. Because this produces a non-diagonal mass matrix, in order to perform decay calculations we must diagonalise to the mass-eigenvalue basis. We write the up-type mass matrix as follows:

$$M_u = M_u^0 + \delta M_u \equiv \begin{pmatrix} m_{cc} & 0 & 0 \\ 0 & m_{tt} & 0 \\ 0 & 0 & \mu_T \end{pmatrix} + \begin{pmatrix} 0 & m_{ct} & m_{cT} \\ m_{tc} & 0 & m_{tT} \\ \mu_c & \mu_t & 0 \end{pmatrix} , \quad (45)$$

which will allow us to use a perturbative approach in $m_{offdiag}/m_{diag}$ to find the diagonalising matrices. The resulting left-handed diagonalization matrix, V_L^u , is given by

$$V_L^u = \begin{pmatrix} 1 & \frac{m_{ct}m_{tt}+m_{cc}m_{ct}+m_{cT}m_{tT}}{m_{tt}^2-m_{cc}^2} & \frac{\mu_T m_{cT} + \mu_c m_{cc} + \mu_t m_{ct}}{\mu_T^2 - m_{cc}^2} \\ \frac{m_{ct}m_{tt}+m_{cc}m_{ct}+m_{cT}m_{tT}}{m_{cc}^2-m_{tt}^2} & 1 & \frac{\mu_T m_{tT} + \mu_c m_{ct} + \mu_t m_{tt}}{\mu_T^2 - m_{tt}^2} \\ \frac{\mu_T m_{cT} + \mu_c m_{cc} + \mu_t m_{ct}}{m_{cc}^2 - \mu_T^2} & \frac{\mu_T m_{tT} + \mu_c m_{ct} + \mu_t m_{tt}}{m_{tt}^2 - \mu_T^2} & 1 \end{pmatrix} . \quad (46)$$

Using the relation $V_L^{u\dagger} M_u M_u^\dagger V_L^u$ in order to determine V_L^u . Similarly, V_R^u is found to be

$$V_R^u = \begin{pmatrix} 1 & \frac{m_{ct}m_{tt}+m_{cc}m_{ct}+\mu_c\mu_t}{m_{tt}^2-m_{cc}^2} & \frac{\mu_T\mu_c+m_{cT}m_{cc}+m_{tT}m_{ct}}{\mu_T^2-m_{cc}^2} \\ \frac{m_{ct}m_{tt}+m_{cc}m_{ct}+\mu_c\mu_t}{m_{cc}^2-m_{tt}^2} & 1 & \frac{m_{ct}m_{cT}+\mu_t\mu_T+m_{tt}m_{tT}}{\mu_T^2-m_{tt}^2} \\ \frac{\mu_T\mu_c+m_{cT}m_{cc}+m_{tT}m_{ct}}{m_{cc}^2-\mu_T^2} & \frac{m_{ct}m_{cT}+\mu_t\mu_T+m_{tt}m_{tT}}{m_{tt}^2-\mu_T^2} & 1 \end{pmatrix}. \quad (47)$$

Given that $V_L^{u\dagger} M_u V_R^u$ diagonalises M_u to M_u^{diag} , we can look at the mass terms

$$\begin{aligned} \mathcal{L}_{mass} &= (\bar{c}'_L \quad \bar{t}'_L \quad \bar{T}'_{\bar{R}}) M_{diag} \begin{pmatrix} c'_R \\ t'_R \\ T'_R \end{pmatrix} \\ &= (\bar{c}'_L \quad \bar{t}'_L \quad \bar{T}'_{\bar{R}}) V_L^{u\dagger} M_u V_R^u \begin{pmatrix} c'_R \\ t'_R \\ T'_R \end{pmatrix} \end{aligned} \quad (48)$$

such that the mass eigenstates are given by

$$\begin{aligned} c'_L &= c_L + \left[\frac{m_{ct}m_{tt} + m_{cc}m_{ct} + m_{cT}m_{tT}}{m_{tt}^2 - m_{cc}^2} \right] t_L + \left[\frac{\mu_T m_{cT} + \mu_c m_{cc} + \mu_t m_{ct}}{\mu_T^2 - m_{cc}^2} \right] T_{\bar{R}} \\ t'_L &= \left[\frac{m_{ct}m_{tt} + m_{cc}m_{ct} + m_{cT}m_{tT}}{m_{cc}^2 - m_{tt}^2} \right] c_L + t_L + \left[\frac{\mu_T m_{tT} + \mu_c m_{ct} + \mu_t m_{tt}}{\mu_T^2 - m_{tt}^2} \right] T_{\bar{R}} \\ T'_{\bar{R}} &= \left[\frac{\mu_T m_{cT} + \mu_c m_{cc} + \mu_t m_{ct}}{m_{cc}^2 - \mu_T^2} \right] c_L + \left[\frac{\mu_T m_{tT} + \mu_c m_{ct} + \mu_t m_{tt}}{m_{tt}^2 - \mu_T^2} \right] t_L + T_{\bar{R}} \end{aligned} \quad (49)$$

and

$$\begin{aligned} c'_R &= c_R + \left[\frac{m_{ct}m_{tt} + m_{cc}m_{ct} + \mu_c\mu_t}{m_{tt}^2 - m_{cc}^2} \right] t_R + \left[\frac{\mu_T\mu_c + m_{cT}m_{cc} + m_{tT}m_{ct}}{\mu_T^2 - m_{cc}^2} \right] T_R \\ t'_R &= \left[\frac{m_{ct}m_{tt} + m_{cc}m_{ct} + \mu_c\mu_t}{m_{cc}^2 - m_{tt}^2} \right] c_R + t_R + \left[\frac{m_{ct}m_{cT} + \mu_t\mu_T + m_{tt}m_{tT}}{\mu_T^2 - m_{tt}^2} \right] T_R \\ T'_R &= \left[\frac{\mu_T\mu_c + m_{cT}m_{cc} + m_{tT}m_{ct}}{m_{cc}^2 - \mu_T^2} \right] c_R + \left[\frac{m_{ct}m_{cT} + \mu_t\mu_T + m_{tt}m_{tT}}{m_{tt}^2 - \mu_T^2} \right] t_R + T_R \end{aligned} \quad (50)$$

The same procedure is followed for the down-type quarks, yielding the same results as above, only with $c \leftrightarrow s$, $t \leftrightarrow b$, $T \leftrightarrow B$.

Higgs sector

Since the mass matrix we wrote above includes vector-like mass terms that do not arise via interaction with the Higgs, there is a misalignment between the mass matrix and the Yukawa interaction matrix. The Lagrangian for the Yukawa interactions with the Higgs is given by

$$\begin{aligned} \mathcal{L}_{Higgs} &= -\lambda_{cc}h\bar{c}_L c_R - \lambda_{ct}h\bar{c}_L t_R - \lambda_{cT}h\bar{c}_L T_R - \lambda_{tc}h\bar{t}_L c_R - \lambda_{tt}h\bar{t}_L t_R - \lambda_{tT}h\bar{t}_L T_R \\ &\quad - \lambda_{ss}h\bar{s}_L s_R - \lambda_{sb}h\bar{s}_L b_R - \lambda_{sB}h\bar{s}_L B_R - \lambda_{bs}h\bar{b}_L s_R - \lambda_{bb}h\bar{b}_L b_R - \lambda_{bB}h\bar{b}_L B_R, \end{aligned} \quad (51)$$

which can be written in matrix form as

$$\begin{aligned}\mathcal{L}_{Higgs} &= -h (\bar{c}_L \quad \bar{t}_L \quad \bar{T}_R) \begin{pmatrix} \lambda_{cc} & \lambda_{ct} & \lambda_{cT} \\ \lambda_{tc} & \lambda_{tt} & \lambda_{tT} \\ 0 & 0 & 0 \end{pmatrix} \begin{pmatrix} c_R \\ t_R \\ T_R \end{pmatrix} + c \leftrightarrow s, \quad t \leftrightarrow b, \quad T \leftrightarrow B \\ &= -h (\bar{c}_L \quad \bar{t}_L \quad \bar{T}_R) \Lambda_u \begin{pmatrix} c_R \\ t_R \\ T_R \end{pmatrix} + c \leftrightarrow s, \quad t \leftrightarrow b, \quad T \leftrightarrow B.\end{aligned}$$

It is clear that applying the same rotation matrices that diagonalised to the mass eigenstate basis will not diagonalise the Yukawa interaction matrix, giving rise to non-zero off-diagonal couplings via the Higgs.

We can write the Lagrangian in terms of the mass eigenstates as

$$\mathcal{L}_{Higgs} = -h (\bar{c}'_L \quad \bar{t}'_L \quad \bar{T}'_R) \Lambda_u^{diag} \begin{pmatrix} c'_R \\ t'_R \\ T'_R \end{pmatrix}, \quad (52)$$

with

$$\Lambda_u^{diag} = V_L^{u\dagger} \Lambda_u V_R^u = \begin{pmatrix} \alpha_{cc} & \alpha_{ct} & \alpha_{cT} \\ \alpha_{tc} & \alpha_{tt} & \alpha_{tT} \\ \alpha_{Tc} & \alpha_{Tt} & \alpha_{TT} \end{pmatrix}, \quad (53)$$

which is not diagonal. The α_{ij} coefficients are listed in Appendix B. They give the size of the mixing through the Higgs between generations in the mass eigenstate basis. To make our expressions more clear, we define quantities $a_i^{u,d}$ where $i = 1, \dots, 6$ in the Appendix, where $a_{1,2,3}^{u,d}$ correspond to the off-diagonal entries in the up (down)-type left diagonalization matrix, and $a_{4,5,6}^{u,d}$ correspond to the right diagonalization matrix.

Electroweak Sector

Due to the addition of the new family of quarks, we must modify the CKM matrix accordingly. The matrix is defined as

$$V_{CKM,(4 \times 4)} = (V_{L,(4 \times 4)}^u)^\dagger V_{L,(4 \times 4)}^d \quad (54)$$

with the full 4×4 matrices approximated as

$$V_{L,(4 \times 4)}^u = \begin{pmatrix} 1 & 0 & 0 & 0 \\ 0 & 1 & a_1^u & a_2^u \\ 0 & -a_1^u & 1 & a_3^u \\ 0 & -a_2^u & -a_3^u & 1 \end{pmatrix}, \quad V_{L,(4 \times 4)}^d = \begin{pmatrix} 1 & 0 & 0 & 0 \\ 0 & 1 & a_1^d & a_2^d \\ 0 & -a_1^d & 1 & a_3^d \\ 0 & -a_2^d & -a_3^d & 1 \end{pmatrix}, \quad (55)$$

where we use the coefficients $a_i^{u,d}$ defined in Appendix B, and explained above, such that the new CKM matrix is approximately given by

$$V_{CKM,(4 \times 4)} = \begin{pmatrix} 1 & 0 & 0 & 0 \\ 0 & 1 + a_1^u a_1^d + a_2^u a_2^d & -a_1^u + a_1^d + a_2^u a_3^d & -a_2^u + a_2^d - a_1^u a_3^d \\ 0 & a_1^u - a_1^d + a_3^u a_2^d & 1 + a_1^u a_1^d + a_3^u a_3^d & -a_3^u + a_3^d + a_1^u a_2^d \\ 0 & a_2^u - a_2^d - a_3^u a_2^d & a_1^u - a_3^d + a_2^u a_1^d & 1 + a_2^u a_2^d + a_3^u a_3^d \end{pmatrix}. \quad (56)$$

Because we did not include the first generation earlier, we have approximated $V_{us}, V_{ub}, V_{cd}, V_{td} = 0$, but doing a full 4×4 analysis would generate these properly as required.

Flavour changing neutral currents (FCNCs) may arise through couplings to the Z boson at tree level. The quark neutral current is given by

$$j_{NC}^\mu = \frac{g}{\cos\theta_W} \sum_i \bar{q}_L^i \gamma^\mu [t_3^i - \sin^2\theta_W Q_i] q_L^i + \bar{q}_R^i \gamma^\mu [-\sin^2\theta_W Q_i] q_R^i. \quad (57)$$

The right handed current does not change with the addition of the T_R state, as it carries the same charge as the other up-type quarks. However, the addition of the $T_{\bar{R}}$ singlet to the left handed states will result in flavour-changing neutral currents, as it does not carry the same isospin as the other left handed quarks. This can be seen by writing down the current in matrix form as

$$\mathcal{L}_{NC} = \frac{g}{\cos\theta_W} (\bar{c}_L \quad \bar{t}_L \quad \bar{T}_{\bar{R}}) \gamma^\mu Z_\mu \left\{ \begin{pmatrix} \frac{1}{2} - \frac{2}{3} \sin^2\theta_W & 0 & 0 \\ 0 & \frac{1}{2} - \frac{2}{3} \sin^2\theta_W & 0 \\ 0 & 0 & \frac{1}{2} - \frac{2}{3} \sin^2\theta_W \end{pmatrix} + \begin{pmatrix} 0 & 0 & 0 \\ 0 & 0 & 0 \\ 0 & 0 & -\frac{1}{2} \end{pmatrix} \right\} \begin{pmatrix} c_L \\ t_L \\ T_{\bar{R}} \end{pmatrix}. \quad (58)$$

This allows it to be seen that there will be a FCNC induced due to the appearance of the $-\frac{1}{2}$ in the matrix (henceforth denoted as $\delta g_{Z\bar{q}q}$ added to the diagonal matrix, which accounts for the isospin of the $T_{\bar{R}}$ being 0). It is then quite clear that the matrix entries for our FCNC will be given by $\beta = g_{Z\bar{q}q} + V_L^\dagger \delta g_{Z\bar{q}q} V_L$, and is found to be:

$$\beta = \begin{pmatrix} \beta_{11} & \beta_{12} & \beta_{13} \\ \beta_{21} & \beta_{22} & \beta_{23} \\ \beta_{31} & \beta_{32} & \beta_{33} \end{pmatrix}, \quad (59)$$

where the coefficients β_{ij} are defined in Appendix B, and give the sizes of the modified interactions between the Z boson and the SM and vector-like quark. Thus the interaction Lagrangian can be written as

$$\mathcal{L}_{NC} = \frac{g}{\cos\theta_W} (\bar{c}'_L \quad \bar{t}'_L \quad \bar{T}'_{\bar{R}}) \gamma^\mu Z_\mu \beta \begin{pmatrix} c'_L \\ t'_L \\ T'_{\bar{R}} \end{pmatrix}. \quad (60)$$

We have shown here the analysis for the up-type sector, and a similar analysis follows for the down-type sector.

4.2 Computation of decay widths

Having introduced these small couplings between the 3rd generation SM quarks and the VL quarks, we now want to check that there is prompt decay via W to b, or H to t, while also ensuring minimal effects on the gluon fusion rate and the diphoton production rate. The Lagrangian term governing the decay of the T to a W boson and b quark is given by $\mathcal{L} = \frac{g}{\sqrt{2}} W_\mu^+ \bar{T}_{\bar{R}} \gamma^\mu V_{Tb} b_L$. This generates the decay partial width

$$\Gamma(T \rightarrow Wb) = \frac{g^2 |V_{Tb}|^2 M_T^3}{8M_W^2} \frac{1}{8\pi} \left(1 - \frac{M_W^2}{M_T^2}\right)^2 \left(1 + \frac{2M_W^2}{M_T^2}\right), \quad (61)$$

where we can see that this will depend on $|V_{Tb}|^2$. We denote the fermion mass eigenvalues as M_t and M_T . For the decay of the T to a Z and a SM top, the Lagrangian term is $\mathcal{L} = \frac{g}{\cos\theta_W} Z_\mu \bar{T}_R \gamma^\mu \beta_{32} t_L$. This generates the decay partial width

$$\Gamma(T \rightarrow Zt) = \frac{g^2 |\beta_{32}|^2 M_T}{4M_Z^2 \cos^2 \theta_W} \frac{1}{8\pi} [(M_T^2 - (M_t + M_Z)^2)(M_T^2 - (M_t - M_Z)^2)]^{1/2} \cdot \left[\frac{M_Z^2}{M_T^2} \left(1 + \frac{M_t^2 - M_Z^2}{M_T^2} \right) + \left(1 - \frac{2M_t^2}{M_T^2} + \frac{M_t^4 - M_Z^4}{M_T^4} \right) \right]. \quad (62)$$

We can see that this depend on β_{32}^2 . For a T decaying to a SM top and a Higgs, the Lagrangian term is $\mathcal{L} = -\alpha_{tT} h \bar{t}_L T_R$. This leads to the decay partial width

$$\Gamma(T \rightarrow Ht) = \frac{\alpha_{tT}^2}{32\pi M_T} [(M_T^2 - (M_t + M_H)^2)(M_T^2 - (M_t - M_H)^2)]^{1/2} \left(1 + \frac{M_t^2 - M_H^2}{M_T^2} \right). \quad (63)$$

So this depends on α_{tT}^2 .

4.3 Experimental Limits from VLQuark searches

In this section we review the current experimental limits from ATLAS and CMS on searches for vector-like quarks, taking the example of a top-like quark. The decays of such a vector-like quark have a dependence on the off-diagonal Yukawa couplings of the T to the t , as well as the other off-diagonal couplings (see definition of α_{tT} in Appendix B). The decay of T to tH will provide a bound on $(\lambda_{tT}^2 \cdot \mu_T)$, as the decay width is $\Gamma(T \rightarrow Ht) \sim \alpha_{tT}^2 \cdot M_T / (32\pi^2)$, and to leading order in M_t/M_T , we have $\alpha_{tT} \sim \lambda_{tT}$ and $M_T \sim \mu_T$, such that $\Gamma(T \rightarrow Ht) \sim \lambda_{tT}^2 \cdot \mu_T / (32\pi^2)$. This approximate expression only applies for $M_T \gg M_t$ (see Eq. (63)), and $\lambda_{ij} \ll 1$ for $i \neq j$. The condition $\lambda_{ij} \ll 1$ comes from the expression for M_T as a function of λ_{ij} that can be seen from Eq. (B.79), recalling that m_{ij} are the masses obtained due to the Higgs VEV in the Yukawa interactions of Sec. 2 such that $m_{ij} = \lambda_{ij} v / \sqrt{2}$.

Depending on the decay width, the decay can either be prompt or displaced. We define a prompt decay to be one where $c\tau < 100\mu\text{m}$, such that it would be smaller than $c\tau$ for the D^0 meson [67], which requires $(\lambda_{tT}^2 \cdot \mu_T) \gtrsim 1.6 \times 10^{-10}$ GeV. Based on 19.6 fb^{-1} , CMS studied the properties of a possible t-like VL quark with decays into bW, tZ and tH. They find limits of between 687 and 782 GeV [76]. The search at ATLAS used 14.3 fb^{-1} of data, with possible t-like decays into bW and tH. They propose limits of between 640 and 790 GeV [77].

If the VL quark is long-lived such that $c\tau \gtrsim 3\text{m}$, it will decay outside the detector, which requires $(\lambda_{tT}^2 \cdot \mu_T) \lesssim 6 \times 10^{-15}$ GeV. Heavy charged long-lived states such as these usually have low, but not zero, energy loss in the detector and may charge oscillate. Limits on long-lived VL quarks can be derived from the interpretation of ATLAS and CMS searches [78]. Using CMS results [79] one can exclude $m_Q < 800$ GeV for $c\tau > 3m$, assuming behaviour similar to that of long-lived heavy scalar top quarks. A caveat is that these limits assume pair-production of the VL quarks, with kinematics independent of the lifetime of the particle [78]. The MoEDAL collaboration discusses [80] in more detail the limits on production cross-section-dependent limits for various decay lifetimes of long-lived VL quarks.

The current FCNC experimental limits also place an upper bound on the off-diagonal Yukawa couplings. In particular, we compute the decay width of $t \rightarrow cX$, where $X = Z, H$ and use that as a means of limiting the mixing between the VL generation and the SM quarks. The current limit on FCNC top decays to a charm and Higgs are given by $\sqrt{|\alpha_{tc}|^2 + |\alpha_{ct}|^2} < 0.14$ [81]. The

current limit on top decays into up-type quarks and Z is given by $BR(t \rightarrow Zq) < 0.05$ [82], with eventual limits expected to reach $BR(t \rightarrow Zq) < 10^{-5}$ [83]. We simplify our analysis by setting all the off-diagonal Yukawa couplings equal to each other, $\lambda_{ij} \equiv \delta$. We find that $\delta \lesssim 0.24$ is required to avoid the constraint on $\sqrt{|\alpha_{tc}|^2 + |\alpha_{ct}|^2}$ for $\mu_T \gtrsim 600$ GeV. This bound comfortably avoids the current bounds set by the decay of the top into Z and an up-type quark.

4.4 Experimental Limits from VLLepton searches

We do not compute limits on vector-like leptons here, so we summarise briefly here the results of Ref. [49]. In the case of singlet vector-like leptons, the constraints are not very tight, with $M_l \gtrsim 100$ GeV if it decays into an electron or muon, and a lower limit less than 100 GeV if it decays into a tau. In the case of doublet vector-like leptons, the constraints are more strict, with $M_l \gtrsim 450$ GeV if it decays into an electron or muon, and $M_l \gtrsim 300$ GeV if it decays into a tau. These lower bounds motivate our choice of lightest mass eigenvalues for the vector-like fermions in Table 2.

5 Higgs Production and Decay Processes

In the SM, the hgg and $h\gamma\gamma$ couplings occur at loop level, the leading order being at one-loop. If vector-like fermions couple to the Higgs boson, they could potentially contribute in these loops and affect these amplitudes. Colored vector-like fermions that couple to the Higgs boson contribute to the $gg \rightarrow h$ loop amplitude, and electromagnetically charged ones to the $h \rightarrow \gamma\gamma$ loop amplitude. Here we present these contributions. We use leading order expressions since we always deal with ratios of these quantities to corresponding SM ones. These ratios are quite insensitive to higher order corrections; for example, Ref. [84] finds that due to vector-like quarks in a composite-Higgs model, the ratios are changed by at most a few percent. Ref. [85] computes the fermion contribution to the ggh effective coupling using the low-energy Higgs theorem. They show the typical size of modification of this vertex in a few models of new physics. They argue that QCD corrections should largely cancel in the ratio $\Gamma_{gg}/\Gamma_{gg}^{SM}$ where the numerator includes the contribution of heavy new physics.

The $h \rightarrow gg$ partial width at leading order (1-loop) in the SM is given for example in Ref. [86]. vector-like fermions that carry color also contribute to the $h \rightarrow gg$ decay rate while uncolored ones do not. We generalize this result to include the contributions due to vector-like fermions in the fundamental representation of $SU(3)$ (i.e. vector-like quarks), denoted as χ , by rescaling with the Higgs coupling shown below in parenthesis (...) as

$$\Gamma(h \rightarrow gg) = \frac{G_\mu \alpha_s^2 m_h^3}{36\sqrt{2}\pi^3} \left| \frac{3}{4} \sum_Q \left(\frac{\kappa_{hQQv}}{\sqrt{2}M_Q} \right) A_{1/2}^h(\tau_Q) \right|^2, \quad (64)$$

where $\tau_Q = m_h^2/4M_Q^2$, Q now includes the SM and the new vector-like quarks, κ_{hQQ} are the Higgs couplings to the quarks, i.e. the usual Yukawa couplings for the SM quarks and the couplings shown in Eqs. (19), (26) and (35) for the new vector-like quarks \mathcal{X} . The function $A_{1/2}$ can be found in Ref. [86]. The rescaling is as shown above since the SM hgg and $h\gamma\gamma$ fermion contributions are proportional to the fermion Yukawa coupling. Also, such a rescaling of the SM (chiral) result is applicable in the vector-like case since a vector-like Weyl fermion pair counts as a Dirac fermion, similar to the SM situation, and the γ and the g interactions are vector-like with respect to the corresponding unbroken gauge-group and do not see the distinction between chiral and vector-like

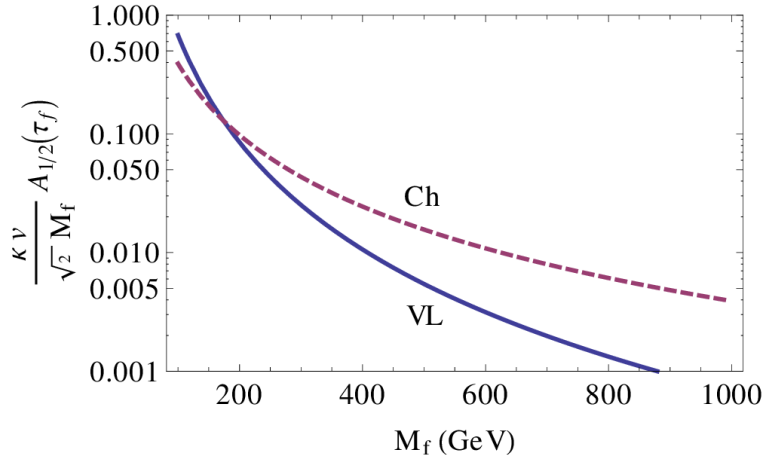


Figure 3: The hgg and $h\gamma\gamma$ triangle loop quantity $\kappa_{hff}v/(\sqrt{2}M_f) A_{1/2}(\tau_f)$ showing how it decouples as a function of M_f , contrasting the vector-like case marked “VL” taking $\kappa_{hff} = 1$ with the chiral case marked “Ch” taking $\kappa_{hff} = \sqrt{2}M_f/v$.

fermions. For our numerical analysis, we take α_s at the scale M_Z . The $gg \rightarrow h$ production can be obtained from the $h \rightarrow gg$ decay rate. At leading order this is (see for example, Ref. [87])

$$\sigma(gg \rightarrow h) = \frac{8\pi^2}{m_h^3} \Gamma(h \rightarrow gg) . \quad (65)$$

The $h\gamma\gamma$ decay rate at leading order (1-loop) in the SM is given for example in Ref. [86]. All states that couple to the Higgs and have nonzero electromagnetic charge contribute to this process. We generalize this result to include the contributions due to vector-like fermions (i.e. vector-like quarks and leptons), denoted as χ , by rescaling with the Higgs coupling shown below in parenthesis (...) as

$$\Gamma(h \rightarrow \gamma\gamma) = \frac{G_\mu \alpha^2 m_h^3}{128\sqrt{2}\pi^3} \left| \sum_f N_c Q_f^2 \left(\frac{\kappa_{hff}v}{\sqrt{2}M_f} \right) A_{1/2}^h(\tau_f) + A_1^h(\tau_W) \right|^2 , \quad (66)$$

where $\tau_i = m_i^2/4M_i^2$, f now includes the SM and the new vector-like fermions, κ_{hff} are the Higgs couplings to fermions, i.e. the usual Yukawa couplings for the SM fermions and the couplings shown in Eqs. (19), (26) and (35) for the new vector-like fermions \mathcal{X} . The function $A_{1/2}$ and A_1 can be found in Ref. [86]. All EM charged fermions, both colored and uncolored, contribute here; $N_c = 3$ for quarks as usual, and abusing notation, $N_c = 1$ for uncolored fermions (leptons). It is noted there that in the $h\gamma\gamma$ amplitude, since the photon is real, one takes $\alpha_{EM}(q^2 = 0)$.

To study the decoupling behavior of the fermion contributions to the ggh and $\gamma\gamma h$ loop amplitudes, we plot in Fig. 3 the quantity $\kappa_{hff}v/(\sqrt{2}M_f) A_{1/2}(\tau_f)$ that appear in Eqs. (64) and (66) contrasting the vector-like case (marked “VL”) with the chiral case (marked “Ch”). For the vector-like case, we fix $\kappa_{hff} = 1$ and M_f varied, while for the chiral case we take $\kappa = \sqrt{2}M_f/v$ since M_f entirely arises from the Yukawa coupling. In fact, the existence of a chiral fourth generation increases the $gg \rightarrow h$ production rate by a factor of 9 compared to the SM, and after including the contribution to the $h \rightarrow \gamma\gamma$ BR, a fourth generation appears to be severely disfavored [88] in a single Higgs doublet model.

Another Higgs production channel is via vector-boson fusion. Although the signal cross-section is lower than Higgs production via gluon fusion, the presence of the forward tagging jets help suppress background, making this mode also promising. We will separate the Higgs production in these categories by including ggh and VBF superscripts respectively. For brevity, we denote $\Gamma_{h \rightarrow XX}$ as Γ_{XX} , etc.

The ‘‘signal strength’’ for the $h \rightarrow XX$ decay mode is defined as

$$\mu_{XX} \equiv \frac{[\sigma(pp \rightarrow h) * BR(h \rightarrow XX)]}{[\sigma(pp \rightarrow h) * BR(h \rightarrow XX)]_{SM}} . \quad (67)$$

Processes that have contributions at the tree-level are modified at loop-level by a relatively small amount, and therefore the contributions of heavy vector-like fermions to such processes can be neglected. For instance, $\Gamma_{ZZ} \approx \Gamma_{ZZ}^{SM}$, $\sigma^{VBF} \approx \sigma_{SM}^{VBF}$, etc. Furthermore, with heavy vector-like fermions present, the total Higgs decay width remains dominated by tree-level decays as it is in the SM, and to a very good approximation, $\Gamma_{tot} \approx \Gamma_{tot}^{SM}$. Thus, in the case of heavy vector-like fermion extensions of the SM, these imply the approximate relations

$$\mu_{\gamma\gamma}^{VBF} \approx \frac{\Gamma_{\gamma\gamma}}{\Gamma_{\gamma\gamma}^{SM}} ; \quad \mu_{ZZ}^{ggh} \approx \frac{\Gamma_{gg}}{\Gamma_{gg}^{SM}} ; \quad \mu_{\gamma\gamma}^{ggh} \approx \frac{\Gamma_{gg}}{\Gamma_{gg}^{SM}} \frac{\Gamma_{\gamma\gamma}}{\Gamma_{\gamma\gamma}^{SM}} ; \quad \frac{\mu_{\gamma\gamma}^{ggh}}{\mu_{ZZ}^{ggh}} \approx \frac{\Gamma_{\gamma\gamma}}{\Gamma_{\gamma\gamma}^{SM}} \approx \mu_{\gamma\gamma}^{VBF} . \quad (68)$$

6 Numerical Results for Electroweak and Higgs Boson Observables

Here we explore the possible impact of vector-like fermions on precision electroweak observables and LHC Higgs observables. We begin with some general comments. Whenever μ_{ZZ} deviates from 1, it is entirely due to the vector-like quark contributions to the ggh vertex as the hZZ vertex is not shifted from its tree-level value. Thus when there are no vector-like quarks present $\mu_{ZZ} = 1$, which for instance is the case with only vector-like leptons present. In the latter case, $\mu_{\gamma\gamma}$ may be shifted. μ_{ZZ} , μ_{WW} and μ_{bb} are all equal to each other since all of them measure the ggh vertex. In the following subsections we present some illustrative examples and show the deviations in $\mu_{\gamma\gamma}$ and μ_{ZZ} we find in the various models presented.

In all the models we consider, the vector-like quark contribution adds constructively with the SM top contribution and increases the magnitude of the ggh vertex when compared to the SM; as a consequence, $\mu_{ZZ,WW,bb} \geq 1$ always. The $h\gamma\gamma$ coupling receives a contribution from the W^\pm as well which is larger and of opposite sign to the SM quark/lepton contribution. The vector-like fermion contribution being of the same sign as the SM quark/lepton contribution therefore decreases the magnitude of the $h\gamma\gamma$ coupling when compared to the SM; as a consequence, $\mu_{\gamma\gamma}^{VBF} \leq 1$ always. $\mu_{\gamma\gamma}^{ggh}$ being the product of the above two (see Eq. (68)) can be either bigger than or lesser than 1.

We argued below Eqs. (4) and (9) that the sign of the Yukawa couplings are not physical in the limit of negligibly small Yukawa couplings mixing SM fermions with vector-like fermions, as we take here. We demonstrate this here explicitly by taking the Υ model as an example. For this, we use the argument for how various quantities change under $\lambda_\Upsilon \rightarrow -\lambda_\Upsilon$ we gave below Eq. (19). It is easy to see that in the vector-like fermion triangle-loop diagrams for $h\gamma\gamma$ and hgg couplings, there are either zero or two couplings that change sign in a particular diagram, thus making the overall sign unchanged. Also, the precision electroweak observables, S, T, U , given in terms of $\Pi_{11}, \Pi_{33}, \Pi_{3Y}$ (and their derivatives with respect to p^2) all depend on s_V^2 , and thus remain unchanged under $\lambda_\Upsilon \rightarrow -\lambda_\Upsilon$. Although we explicitly demonstrate here for the Υ model, this is true for all of the

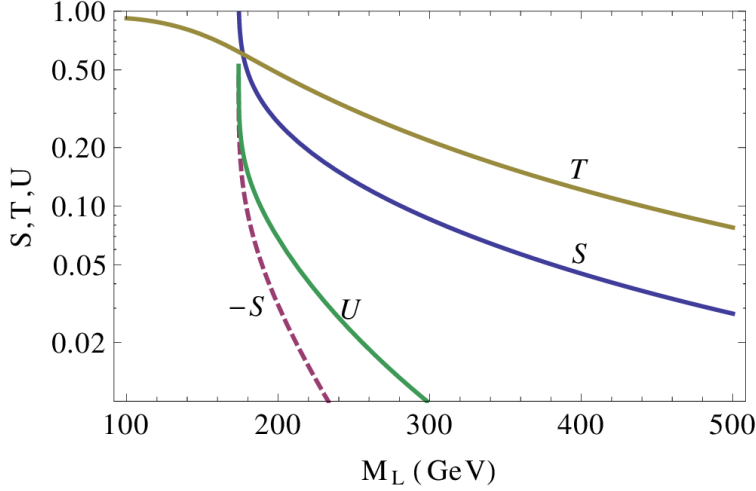


Figure 4: S, T, U for $MVLE_1$ as a function of M_L with $\lambda_E = 1$, $M_E = M_L$, for $Y_L = -1/2$ (solid) and $Y_L = 1/2$ (dashed, for which $-S$ is shown).

models we have discussed in Sec. 2 due to the general arguments given below Eqs. (4) and (9). We therefore restrict ourselves to positive Yukawa couplings in the following, without loss of generality.

6.1 $MVLE_1$ vector-like Leptons Model

In Fig. 4 we show S, T, U as a function of M_L for $MVLE_1$ with $M_E = M_L$ and $\lambda_E = 1$. Note that T and U are independent of Y_L . Furthermore, $U \lesssim 0.02$ for $M_{L,E} > 250$ GeV, and will not place any nontrivial constraints; we therefore ignore U in the rest of our analysis.

For $Y_L = 1/2$ ($-1/2$), the χ_2, χ_3 (χ_1) mass eigenstates are EM neutral (and color singlet) as can be seen from Table 1. These assignments of Y_L are therefore interesting for dark matter if the lightest χ is stable and in regions of parameter space where it is EM neutral. In the $Y_L = 1/2$ ($-1/2$) Υ (ξ) model case, the EM charged state χ_1 (χ_2) does not couple to the Higgs as seen from Eq. (19), (26) and thus $\mu_{\gamma\gamma}$ will be 1. Since there are no new colored fermions, the $gg \rightarrow h$ production is unchanged, and $\mu_{ZZ,WW,bb}$ etc. will also be 1.

We show in Fig. 5 the constraint from S and T parameters and $\mu_{\gamma\gamma}^{ggh}$. S and T are within the 68 % CL ellipse in the light gray region, between 68 % and 95 % ellipse in the medium gray region, and excluded worse than 95 % CL in the dark gray region. We also show the (100, 250, 450) GeV contours (with boxed numbers) of the the minimum mass eigenvalue, i.e. $\min(m_1, m_2, m_3)$. It is possible that in some specially constructed models such light masses may still be allowed; for a discussion of the limits on vector-like leptons, see for example Ref. [49]. To the left of the black solid line there is a mass eigenvalue < 250 GeV. Therefore the safest region in most models from both S and T parameters and from direct collider constraints is the light gray region to the right of all black lines. With only vector-like leptons added, the hgg coupling is unaltered and the deviations of interest are all in the $h\gamma\gamma$ coupling. Thus, $\mu_{\gamma\gamma}^{ggh}$ is altered as shown, whereas $\mu_{ZZ,bb}^{ggh} = 1$ and $\Gamma_{gg} = \Gamma_{gg}^{SM}$ and are not shown.

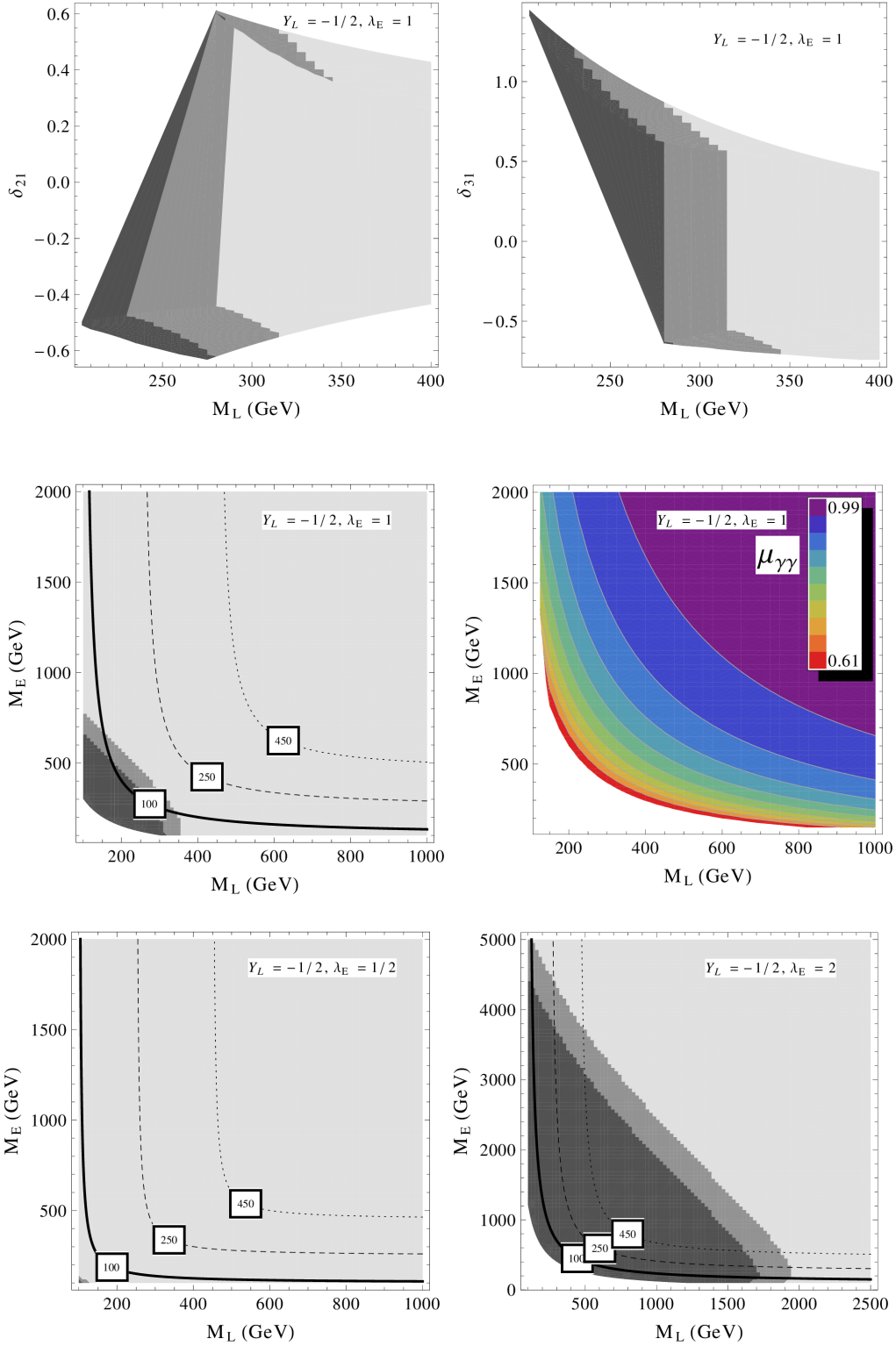


Figure 5: For the MVLE₁ model with $Y_L = -1/2$, $\lambda_E = 0.5$ (first four figures) and $\lambda_E = 1$ (bottom-left), $\lambda_E = 2$ (bottom-right), S and T allowed regions are shown in all the plots, except middle-right which shows the $\mu_{\gamma\gamma}^{gh}$ (in which the values increase from bottom-left corner to top-right). S and T are within the 68 % CL ellipse in the light gray region, between 68 % and 95 % ellipse in the medium gray region, and excluded worse than 95 % CL in the dark gray region. The boxed numbers label (in GeV) contours of the minimum mass eigenvalue, i.e. $\min(m_1, m_2, m_3)$.

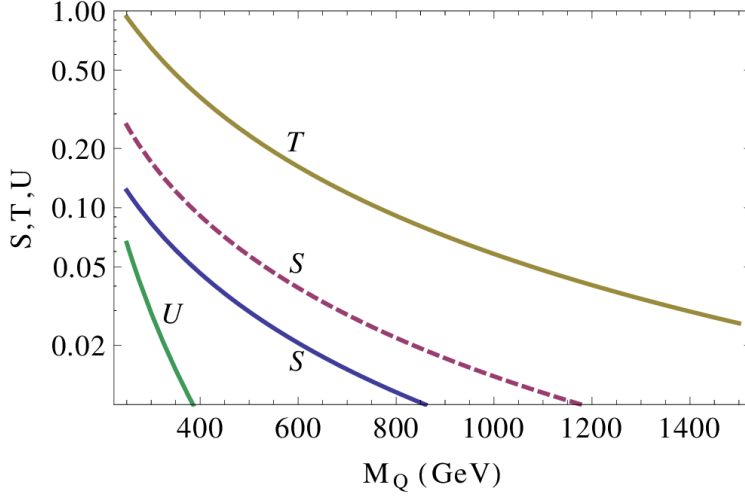


Figure 6: S, T, U for MVQD₁ with $\lambda_D = 1$ and $M_D = M_Q$ for $Y_Q = 1/6$ (solid) and $Y_Q = -1/6$ (dashed).

6.2 MVQD₁ vector-like Quarks Model

In Fig. 6 we show S, T, U as a function of M_Q for MVQD₁. Note that T is always positive and independent of Y_Q . $U \lesssim 0.003$ for $M_{Q,D} > 500$ GeV, and will not place any nontrivial constraints; we therefore ignore U in the rest of our analysis. In Fig. 7 we show the the constraint from S and T parameters as shaded regions for $Y_Q = 1/6, \lambda_D = 0.5, 1, 2$, and for $Y_Q = -1/6, \lambda_D = 1$. We also show the (500, 700) GeV contours (with boxed numbers) of the the minimum mass eigenvalue, i.e. $\min(m_1, m_2, m_3)$. In Fig. 8 we show $\mu_{\gamma\gamma}^{ggh}, \mu_{ZZ}^{ggh}$ and $\mu_{\gamma\gamma}^{ggh}/\mu_{ZZ}^{ggh}$ for $Y_Q = 1/6$ and $-1/6$ for $\lambda_D = 1$. Keeping in mind the direct LHC limits on a vector-like b' and t' we ensure that all mass eigenvalues are > 500 GeV and show them as the colored region. The deviation in μ_{ZZ}^{ggh} is entirely due to a change in the ggh vertex since the hZZ vertex is unchanged, and this change is the same for either sign of Y_Q . In general, in $gg \rightarrow h \rightarrow \gamma\gamma$, i.e. for $\mu_{\gamma\gamma}^{ggh}$, both production and decay vertices are shifted; the ggh vertex is shifted due to the presence of new colored vector-like fermions, and the $h\gamma\gamma$ vertex is shifted since these states carry EM charge as well. Interestingly, as can be seen from Eq. (19), the $h\gamma\gamma$ coupling shift is small in this model since \mathcal{X}_1 does not couple to the h , while the h couplings to \mathcal{X}_2 and \mathcal{X}_3 are opposite sign and will cancel up to mass differences. In all cases, the μ asymptote to 1 as the vector-like fermion contributions decouple.

6.3 VSM₁ vector-like Standard Model

Keeping in mind the direct collider limits, we restrict to the parameter-space with all vector-like quark mass eigenvalue ≥ 500 GeV and lepton mass eigenvalues ≥ 250 GeV. In Fig. 9 we show the signal strength in the VSM₁ with all the vector-like quark and lepton masses equal to the value shown in the X -axis, i.e. $M_{\{Q,U,D,L,E,N\}} = M_{VL}$, with $Y_Q = 1/6$ and $Y_L = -1/2$, and all the Yukawa couplings $\lambda = 1$. All these points satisfy the S and T constraints at or better than 2σ level. The color of the dots denote the lightest mass eigenvalue; the red, blue and green dots respectively stand for light, medium and heavy mass categories given in Table 2. These mass eigenvalue ranges are motivated by the direct collider limits discussed in Sections 4.3 and 4.4. In Fig. 10 we show the μ with all the vector-like quark and lepton masses set equal ($M_{\{Q,U,D,L,E,N\}} = M_{VL}$), and all the

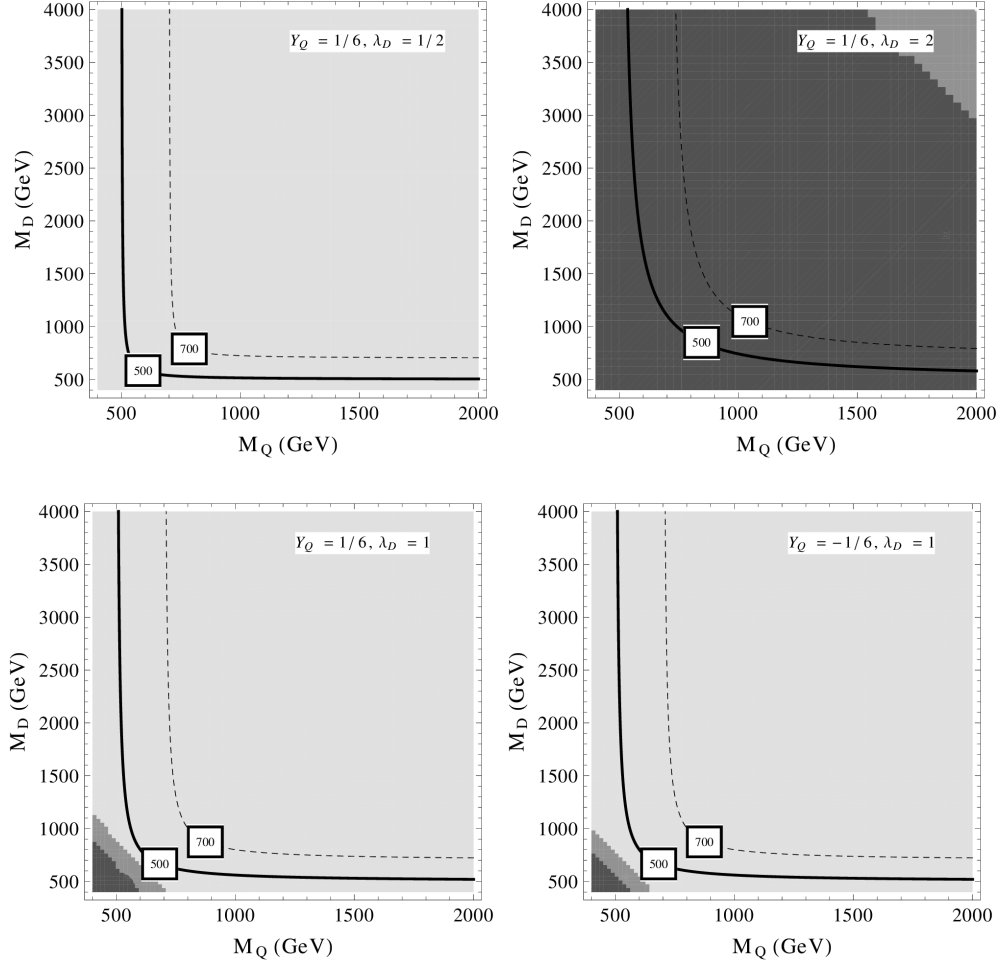


Figure 7: S and T parameters for the MVQD₁ model with $Y_Q = 1/6$, $\lambda_D = 0.5, 1, 2$, and for $Y_Q = -1/6$, $\lambda_D = 1$. S and T are within the 68 % CL ellipse in the light gray region, between 68 % and 95 % ellipse in the medium gray region, and excluded worse than 95 % CL in the dark gray region. The boxed numbers label (in GeV) contours of the minimum mass eigenvalue, i.e. $\min(m_1, m_2, m_3)$.

λ set equal ($\lambda_{\{U,D,E,N\}} = \lambda_{VL}$), for $Y_Q = 1/6$ and $Y_L = -1/2$. All these points satisfy the S and T constraints at or better than 2σ level. The color of the dots denote the lightest mass eigenvalue; the red, blue and green dots respectively stand for light, medium and heavy mass categories given in Table 2.

Next, we present some more results where we perform the scan in a more unconstrained fashion. We show in Fig. 11 the signal strength $\mu_{\gamma\gamma}^{ggh}$, in Fig. 12 the signal strength $\mu_{\gamma\gamma}^{VBF}$, in Fig. 13 the signal strength μ_{ZZ} and in Fig. 14 the correlation between $\mu_{\gamma\gamma}^{ggh, VBF}$ and μ_{ZZ} in the VSM₁ model by scanning over all the vector-like quark and lepton masses in the range (50, 5000) GeV, for $Y_Q = 1/6$ and $Y_L = -1/2$, and the Yukawa couplings in the range (0.1, 5). We set all the quark masses equal, i.e. $M_{\{Q,U,D\}} = M_Q$, and quark Yukawa couplings equal, i.e. $\lambda_U = \lambda_D \equiv \lambda_Q$, and all the lepton masses equal, i.e. $M_{\{L,E,N\}} = M_L$ and all lepton Yukawa couplings equal, i.e. $\lambda_E = \lambda_N \equiv \lambda_L$. All these points satisfy the S and T constraints at or better than 2σ level. The color of the dots denote

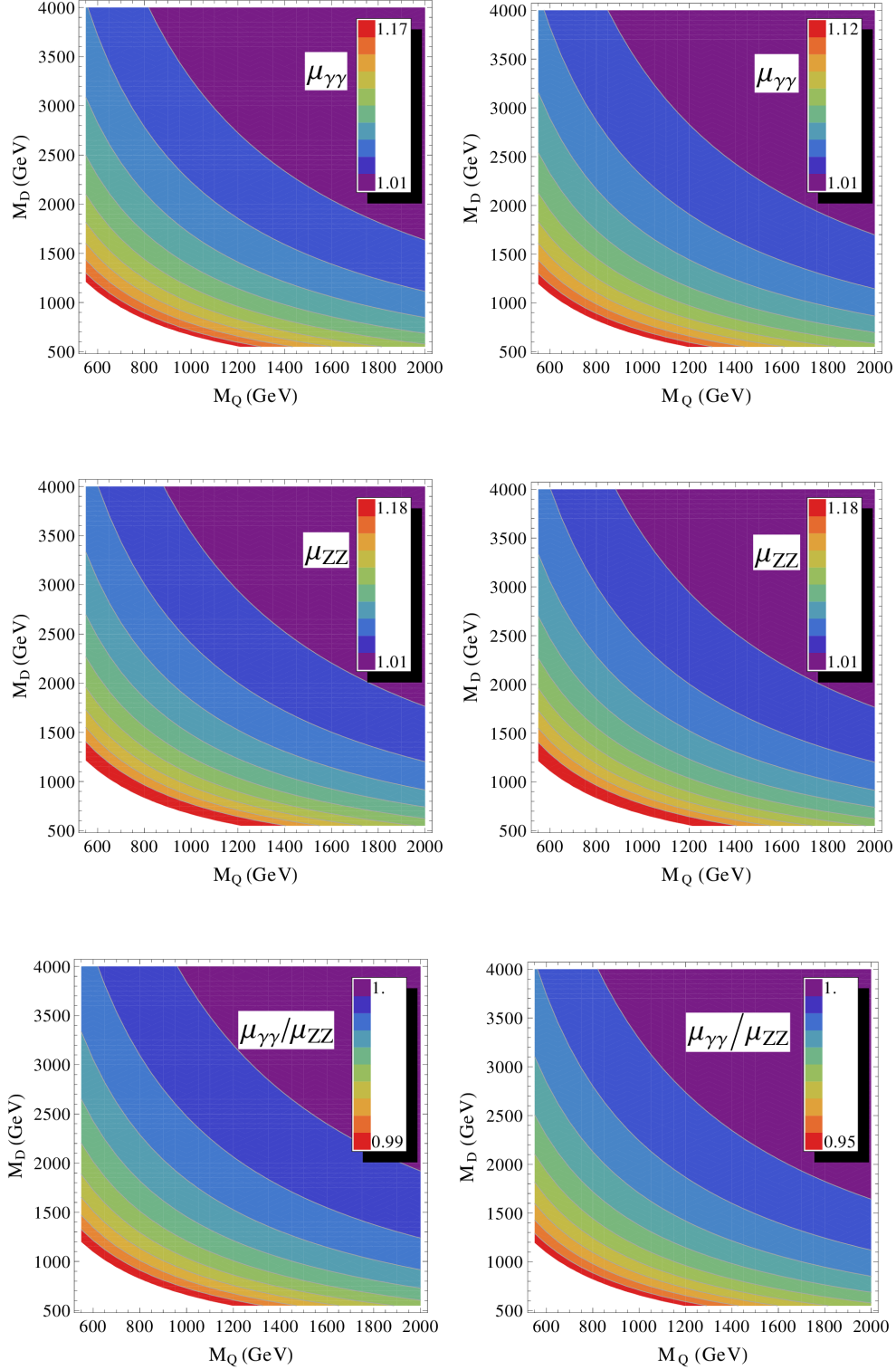


Figure 8: For the MVQD₁ model, $\mu_{\gamma\gamma}^{ggh}$, μ_{ZZ}^{ggh} and $\mu_{\gamma\gamma}^{ggh}/\mu_{ZZ}^{ggh}$ for $\lambda_D = 1$, $Y_Q = 1/6$ (left panel) and $Y_Q = -1/6$ (right panel). The colored region has all mass eigenvalues > 500 GeV. In every plot, the μ values progressively approach 1 as we go toward heavier masses (i.e. top-right corner).

Table 2: The three categories for the lightest mass eigenvalue of the vector-like quark and lepton. “Light” is with *either* the M_q or the M_l as shown, “Medium” is with *each* in the interval shown, and “Heavy” is with *both* above the values shown.

	$M_q(\text{GeV})$	$M_l(\text{GeV})$
Light	≤ 700	≤ 450
Medium	(700, 1000)	(450, 750)
Heavy	> 1000	> 750

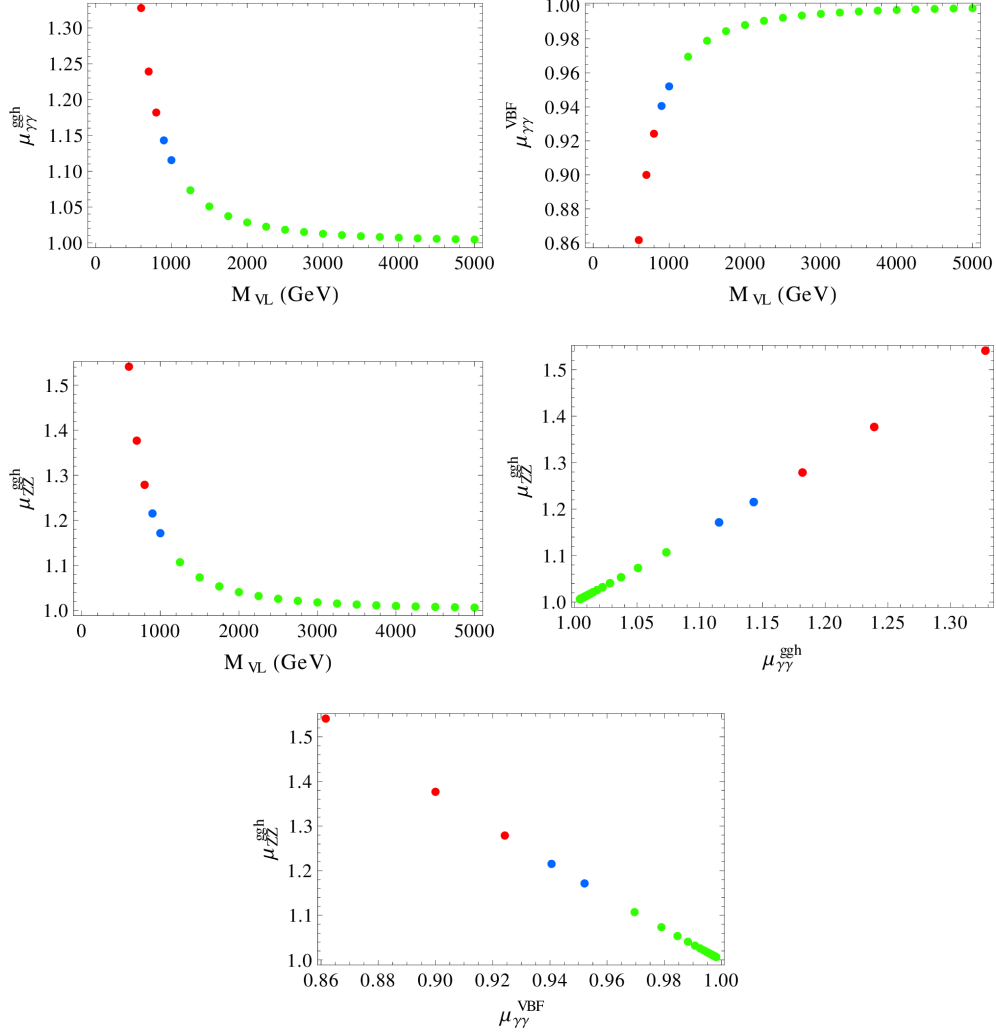


Figure 9: μ in the VSM_1 model with all the vector-like quark and lepton masses equal to the value shown in the X -axis, i.e. $M_{\{Q,U,D,L,E,N\}} = M_{VL}$, with $Y_Q = 1/6$ and $Y_L = -1/2$, and all the Yukawa couplings $\lambda = 1$. All these points satisfy the S and T constraints at or better than 2σ level. The color (or shade of gray, if viewing in gray-scale) of the dots denote the lightest mass eigenvalue; the red (dark gray), blue and green (light gray) dots respectively stand for light, medium and heavy mass categories given in Table 2.

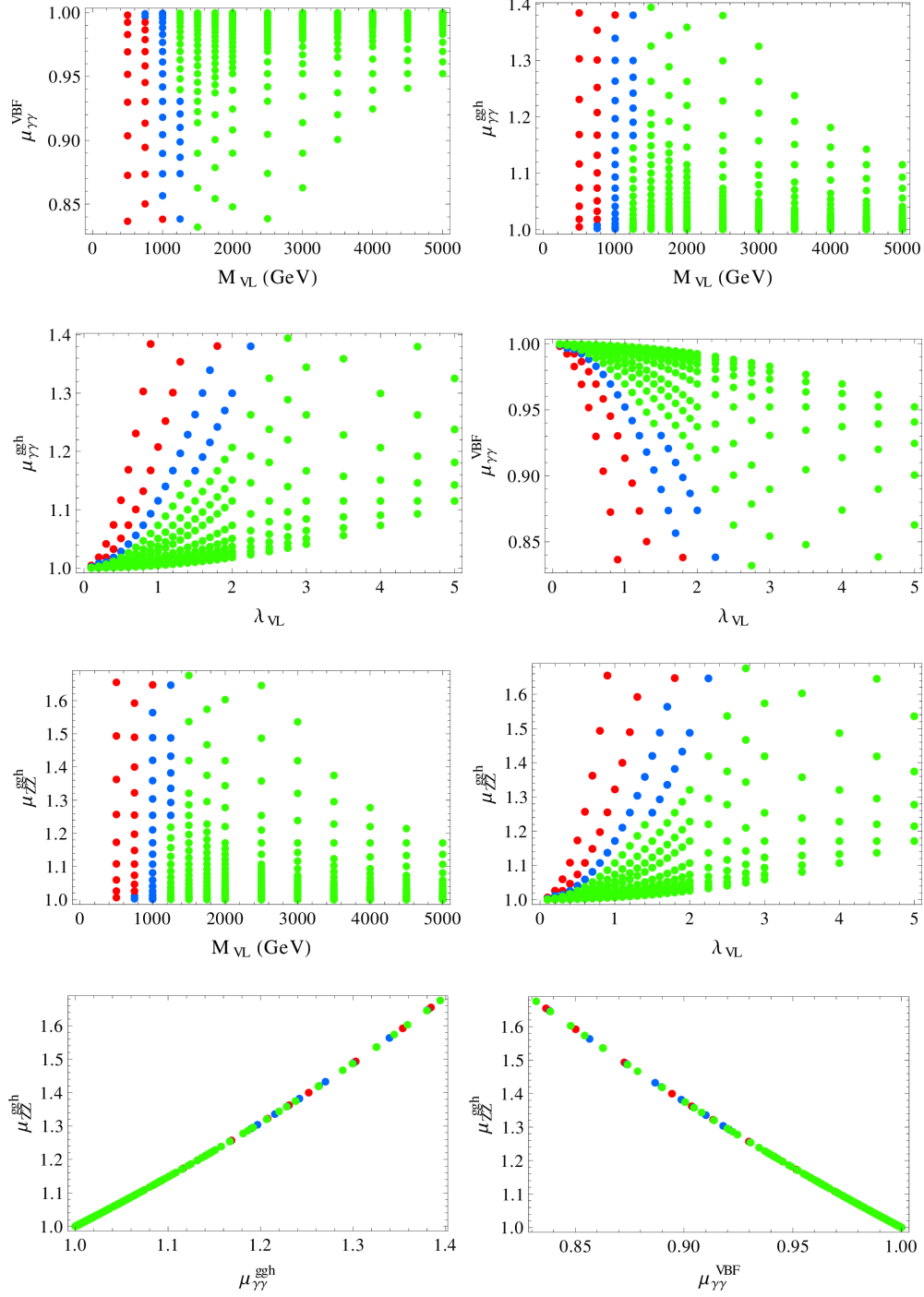


Figure 10: μ in the VSM₁ model with all the vector-like quark and lepton masses set equal ($M_{\{Q,U,D,L,E,N\}} = M_{VL}$), and all the λ set equal ($\lambda_{\{U,D,E,N\}} = \lambda_{VL}$), for $Y_Q = 1/6$ and $Y_L = -1/2$. All these points satisfy the S and T constraints at or better than 2σ level. The color (or shade of gray, if viewing in gray-scale) of the dots denote the lightest mass eigenvalue; the red (dark gray), blue and green (light gray) dots respectively stand for light, medium and heavy mass categories given in Table 2.

the lightest mass eigenvalue; the red, blue and green dots respectively stand for light, medium and heavy mass categories given in Table 2. These results indicate the sizes of the deviations one can

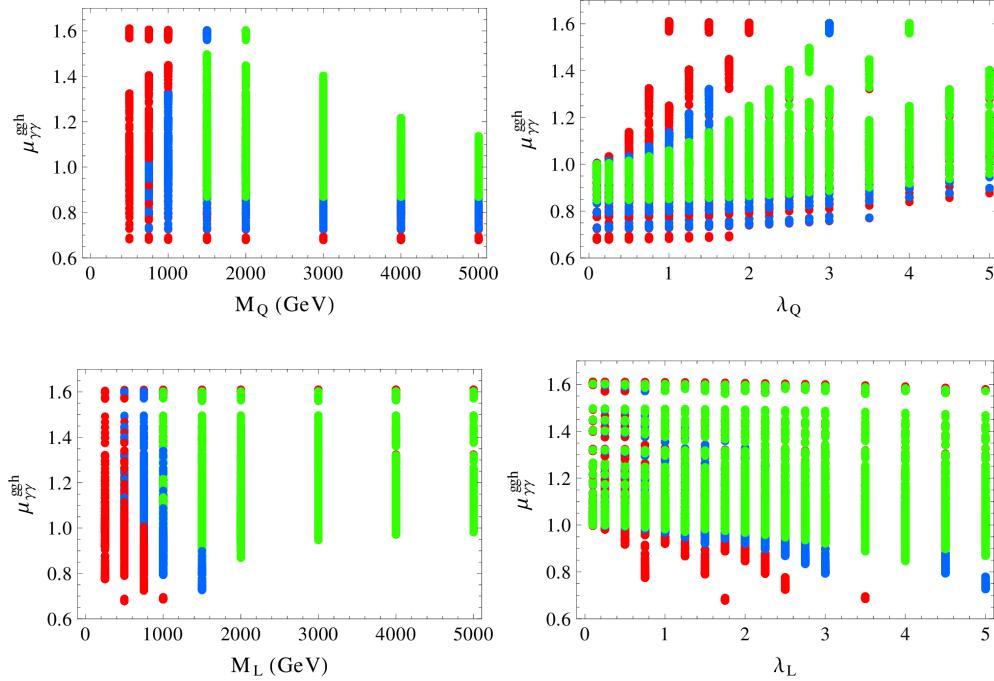


Figure 11: $\mu_{\gamma\gamma}^{ggh}$ in the VSM₁ model from a scan over all the vector-like quark and lepton masses in the range (50, 5000) GeV, and the Yukawa couplings in the range (0.1, 5), with the Q, U, D, L, E, N vector-like fermion fields all present, with $M_Q = M_U = M_D$, $M_L = M_E = M_N$, $\lambda_U = \lambda_D \equiv \lambda_Q$, and $\lambda_E = \lambda_N \equiv \lambda_L$, for $Y_Q = 1/6$ and $Y_L = -1/2$. All the points satisfy the S and T constraints at or better than 2σ level. The color (or shade of gray, if viewing in gray-scale) of the dots denote the lightest mass eigenvalue; the red (dark gray), blue and green (light gray) dots respectively stand for light, medium and heavy mass categories given in Table 2.

expect in the models that we have considered. In the next subsection, we ask to what degree such deviations are allowed by the present LHC Higgs data and the constraints on the model parameter space.

6.4 Fit to the LHC Higgs data

The ATLAS and CMS collaborations have extracted the effective hgg and $h\gamma\gamma$ couplings from a combined fit to the various observed diboson Higgs decay modes. We give this result in Table 3, where we quote the ATLAS result [69] directly as given, while we have translated the CMS result [70] on the 95% C.L intervals of $\kappa_g = [0.63, 1.05]$ and $\kappa_\gamma = [0.59, 1.30]$ to the 1σ values shown. We

Table 3: κ_g and κ_γ values from ATLAS [69] and CMS [70].

Coupling	ATLAS	CMS
κ_g	1.04 ± 0.14	0.83 ± 0.11
κ_γ	1.2 ± 0.15	0.97 ± 0.18

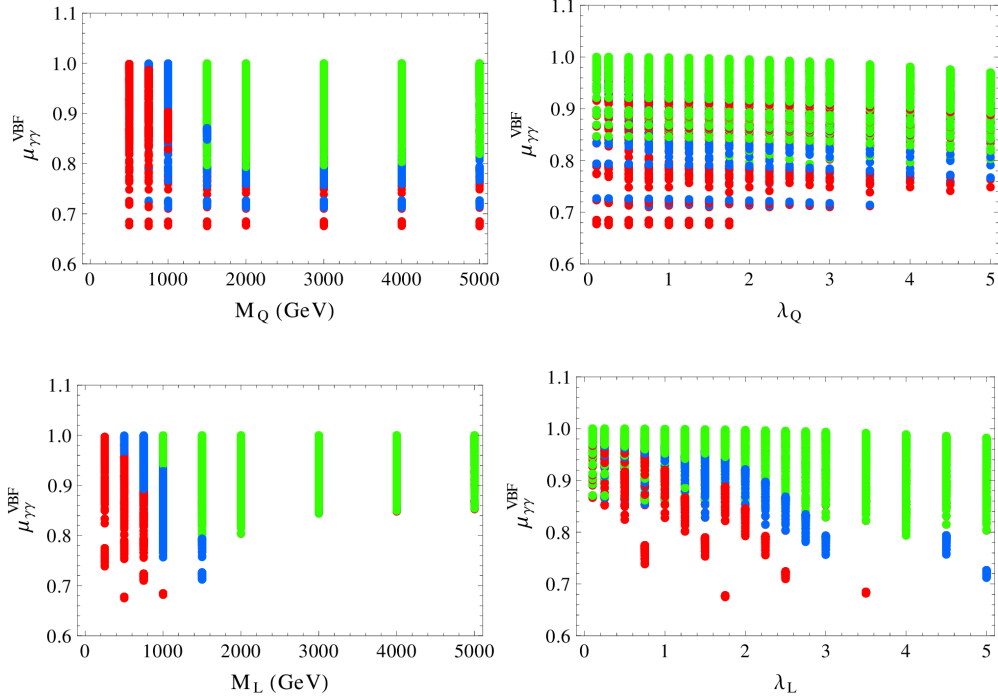


Figure 12: $\mu_{\gamma\gamma}^{VBF}$ in the VSM₁ model from a scan over all the vector-like quark and lepton masses in the range (50, 5000) GeV, and the Yukawa couplings in the range (0.1, 5), with the Q, U, D, L, E, N vector-like fermion fields all present, with $M_Q = M_U = M_D$, $M_L = M_E = M_N$, $\lambda_U = \lambda_D \equiv \lambda_Q$, and $\lambda_E = \lambda_N \equiv \lambda_L$, for $Y_Q = 1/6$ and $Y_L = -1/2$. All the points satisfy the S and T constraints at or better than 2σ level. The color (or shade of gray, if viewing in gray-scale) of the dots denote the lightest mass eigenvalue; the red (dark gray), blue and green (light gray) dots respectively stand for light, medium and heavy mass categories given in Table 2.

perform a χ^2 fit of the SM plus vector-like fermions model to these data. We treat the ATLAS and CMS channels shown in the Table as independent, implying four degrees of freedom (*dof*). We neglect correlations between κ_g and κ_γ , which is a reasonable approximation.

We compute the χ^2 function

$$\chi^2 = \sum_{i=1}^4 \left(\kappa_i^{\text{Exp}} - \kappa_i^{\text{Th}} \right)^2 / \left(\sigma_i^{\text{Exp}} \right)^2, \quad (69)$$

where the $\kappa_i^{\text{Th}} = \{\kappa_g, \kappa_\gamma\}$ for the SM plus vector-like fermion models discussed in Sec. 2, and compared with the respective four κ_i^{Exp} ATLAS and CMS experimental values shown in Table 3. The κ_i are given by

$$\kappa_g = \sqrt{\frac{\Gamma_{gg}}{\Gamma_{gg}^{SM}}} \quad ; \quad \kappa_\gamma = \sqrt{\frac{\Gamma_{\gamma\gamma}}{\Gamma_{\gamma\gamma}^{SM}}}. \quad (70)$$

As is standard (see for example, Ref. [89]), from the χ^2 value for that model with vector-like fermions and the above LHC data (with *dof* = 4), we compute \mathcal{F}_{χ^2} (which is twice the “p-value”), the fraction of times a worse fit is obtained, which is the integral of the tail of the χ^2 distribution from that χ^2 value up to infinity. Roughly speaking, the regions of parameter space where $\mathcal{F}_{\chi^2} < 0.05$ can be

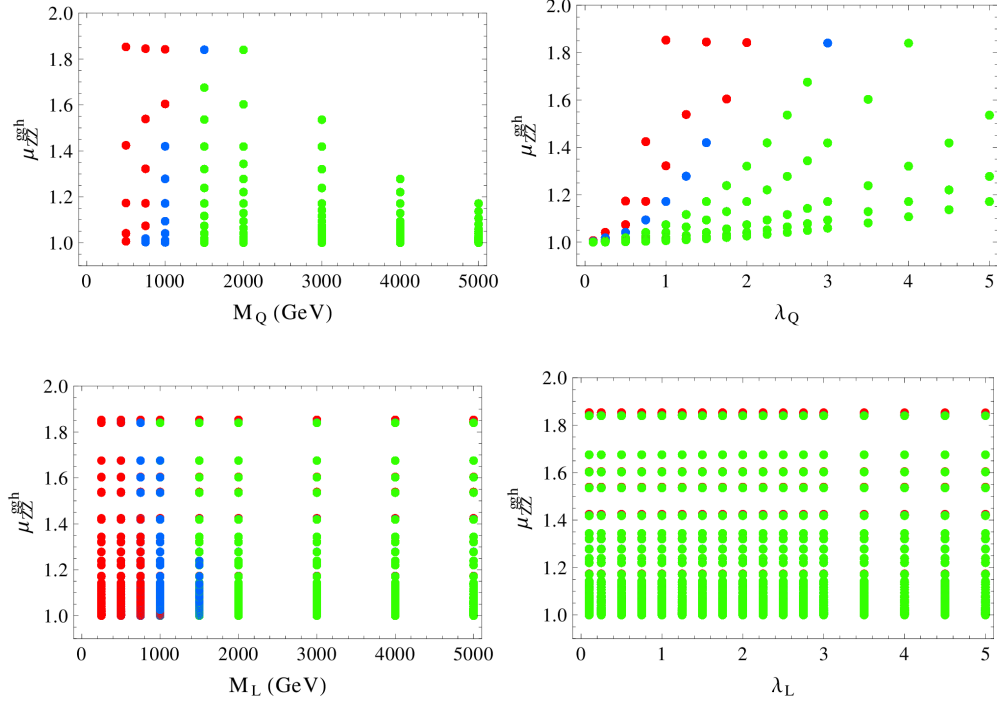


Figure 13: μ_{ZZ} in the VSM₁ model from a scan over all the vector-like quark and lepton masses in the range (50, 5000) GeV, and the Yukawa couplings in the range (0.1, 5), with the Q, U, D, L, E, N vector-like fermion fields all present, with $M_Q = M_U = M_D$, $M_L = M_E = M_N$, $\lambda_U = \lambda_D \equiv \lambda_Q$, and $\lambda_E = \lambda_N \equiv \lambda_L$, for $Y_Q = 1/6$ and $Y_L = -1/2$. All the points satisfy the S and T constraints at or better than 2σ level. The color (or shade of gray, if viewing in gray-scale) of the dots denote the lightest mass eigenvalue; the red (dark gray), blue and green (light gray) dots respectively stand for light, medium and heavy mass categories given in Table 2.

taken to be excluded at about 2σ Gaussian equivalent, and regions where $\mathcal{F}_{\chi^2} < 0.01$ excluded at about 2.6σ .

For the SM alone, without the addition of vector-like fermions, we have $\kappa_{g,\gamma} = 1$ by definition, and from the data in Table 3 we obtain $\chi^2/dof = 1.07$ which yields $\mathcal{F}_{\chi^2} = 0.37$, an acceptable fit to the data. Next, we present χ^2 and \mathcal{F}_{χ^2} for the SM plus vector-like fermions with the goal of identifying regions of vector-like fermion parameter space that have values of \mathcal{F}_{χ^2} bigger than about 0.05, which can be taken as the allowed regions for that model, given the present data.

In Fig. 15 we show the χ^2/dof and \mathcal{F}_{χ^2} for the VL₁ model with $Y_L = -1/2$, $\lambda_{L,N} = 1$, $M_E = M_N$, i.e., the vector-like singlet masses taken equal. The parameter space shown in color is with all lepton mass eigenvalues ≥ 250 GeV, and satisfy the S and T constraints at or better than 2σ .

In Fig. 16 we show the χ^2/dof and \mathcal{F}_{χ^2} for the VQ₁ model with $Y_Q = 1/6$, $\lambda_{U,D} = 1$, $M_U = M_D$, i.e., the vector-like singlet masses taken equal. The parameter space shown in color is with all quark mass eigenvalues ≥ 500 GeV, and satisfy the S and T constraints at or better than 2σ .

In Fig. 17 we show the χ^2/dof and \mathcal{F}_{χ^2} for the VSM₁ model with $Y_Q = 1/6$, $Y_L = -1/2$, $\lambda_{U,D} \equiv \lambda_q = 1$, $\lambda_{E,N} \equiv \lambda_\ell = 1$, $M_{Q,U,D} \equiv M_q = 1000$ GeV, $M_{L,E,N} \equiv M_\ell = 500$ GeV, i.e. all the vector-like quark masses are taken equal, and all the vector-like lepton masses are taken equal (but not necessarily the same as the quark masses). The plots show the dependence on the

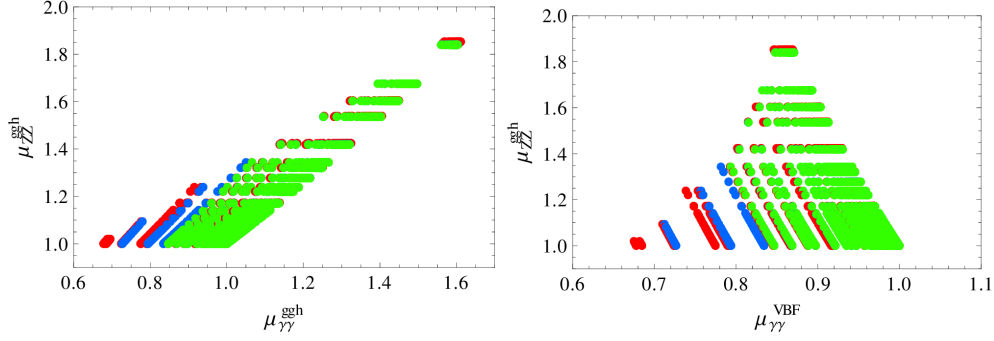


Figure 14: $\mu_{\gamma\gamma}^{ggh, VBF} - \mu_{ZZ}^{ggh}$ correlation in the VSM_1 model from a scan over all the vector-like quark and lepton masses in the range (50, 5000) GeV, and the Yukawa couplings in the range (0.1, 5), with the Q, U, D, L, E, N vector-like fermion fields all present, with $M_Q = M_U = M_D, M_L = M_E = M_N, \lambda_U = \lambda_D \equiv \lambda_Q$, and $\lambda_E = \lambda_N \equiv \lambda_L$, for $Y_Q = 1/6$ and $Y_L = -1/2$. All the points satisfy the S and T constraints at or better than 2σ level. The color (or shade of gray, if viewing in gray-scale) of the dots denote the lightest mass eigenvalue; the red (dark gray), blue and green (light gray) dots respectively stand for light, medium and heavy mass categories given in Table 2.

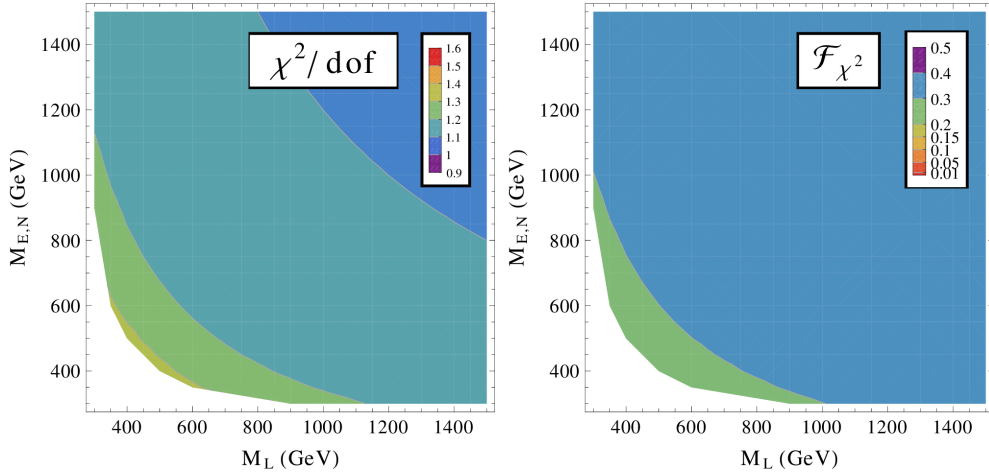


Figure 15: For the VL_1 model, for $Y_L = -1/2, \lambda_E = 1, \lambda_N = 1, M_E = M_N$. The colored regions are with all lepton mass eigenvalues ≥ 250 GeV, and lie within the 2σ ellipse in S and T . In all the plots, χ^2 values decrease and \mathcal{F} values increase as we go toward larger masses, or lower λ .

two parameters that are varied with the other parameters fixed at the above mentioned values. The colored regions are with all quark mass eigenvalues ≥ 500 GeV, all lepton mass eigenvalues ≥ 250 GeV, and satisfy the S and T constraints at or better than 2σ . For given masses, the χ^2 approaches the SM value as λ decreases; for example, for $\lambda = 0.5, M_q = 1000$ GeV, $M_\ell = 500$ GeV we have $\chi^2/\text{dof} = 1.26, \mathcal{F}_{\chi^2} = 0.28$.

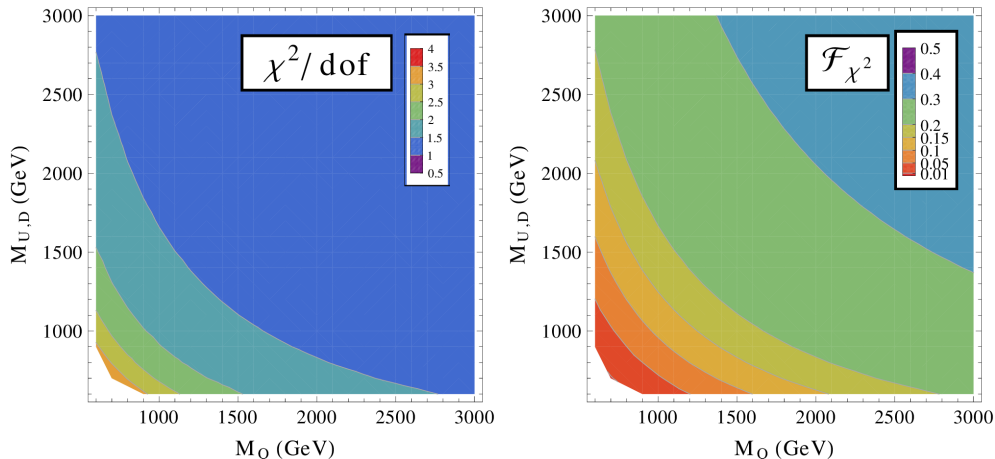


Figure 16: For the VQ_1 model, for $Y_Q = 1/6$, $\lambda_U = 1$, $\lambda_D = 1$, $M_U = M_D$. The colored regions are with all quark mass eigenvalues ≥ 500 GeV, and satisfy the S and T constraints at or better than 2σ . In all the plots, χ^2 values decrease and \mathcal{F} values increase as we go toward larger masses, or lower λ .

7 Conclusions

In this paper we have surveyed numerous vector-like fermion extensions of the SM. Our purpose has been to illuminate the structure of the theories, detail the precision electroweak implications and constraints, investigate LHC direct limits, and investigate the implications of vector-like fermions for Higgs boson production and decay.

The phenomenological implications of vector-like theories depend crucially on the details of the precise theory in question. Precision electroweak constraints depend on masses and couplings to vector bosons, flavor constraints depend on their flavor mixings with SM fermions, direct detection constraints depend on mass hierarchies and the size of the couplings and mixings to SM states that enable prompt or non-prompt decays into various model-specific final state ratios. In addition, the Higgs boson observables depend on overall mass scales and the ratios of the strongly interacting vector-like masses to electroweak interacting states. Our aim was to demonstrate all of these features through examples and extensive computations.

One of the recent motivations for considering vector-like states added to the SM was to account for possible deviations in the $\mu_{\gamma\gamma} = \sigma(h)B(h \rightarrow \gamma\gamma)$ rate at the LHC. As discussed in a Sec. 6.4, early indications from the LHC Higgs studies suggested an enhanced rate to two photons. Presently the central values of the ATLAS data are higher than the SM expected rates, and the central values of the CMS data are lower than the SM expected rates, making a combined total more consistent with the SM than originally thought. Nevertheless, it is one of the few observables that is sensitive to new physics in loops, and the uncertainties in the experimental measurements and QCD uncertainties [90] give plenty of room for large effects (tens of percent) from new physics. In our investigations we have shown that the addition of vector-like fermions with vector-like masses less than a few TeV, and with chiral couplings to the Higgs boson, leads to tens of percent shifts in Higgs production ($gg \rightarrow h \rightarrow XY$) and decay ($h \rightarrow \gamma\gamma$) observables. In time, measurements of Higgs observables and direct searches for vector-like states will go far to confirm or exclude this possibility near the weak scale.

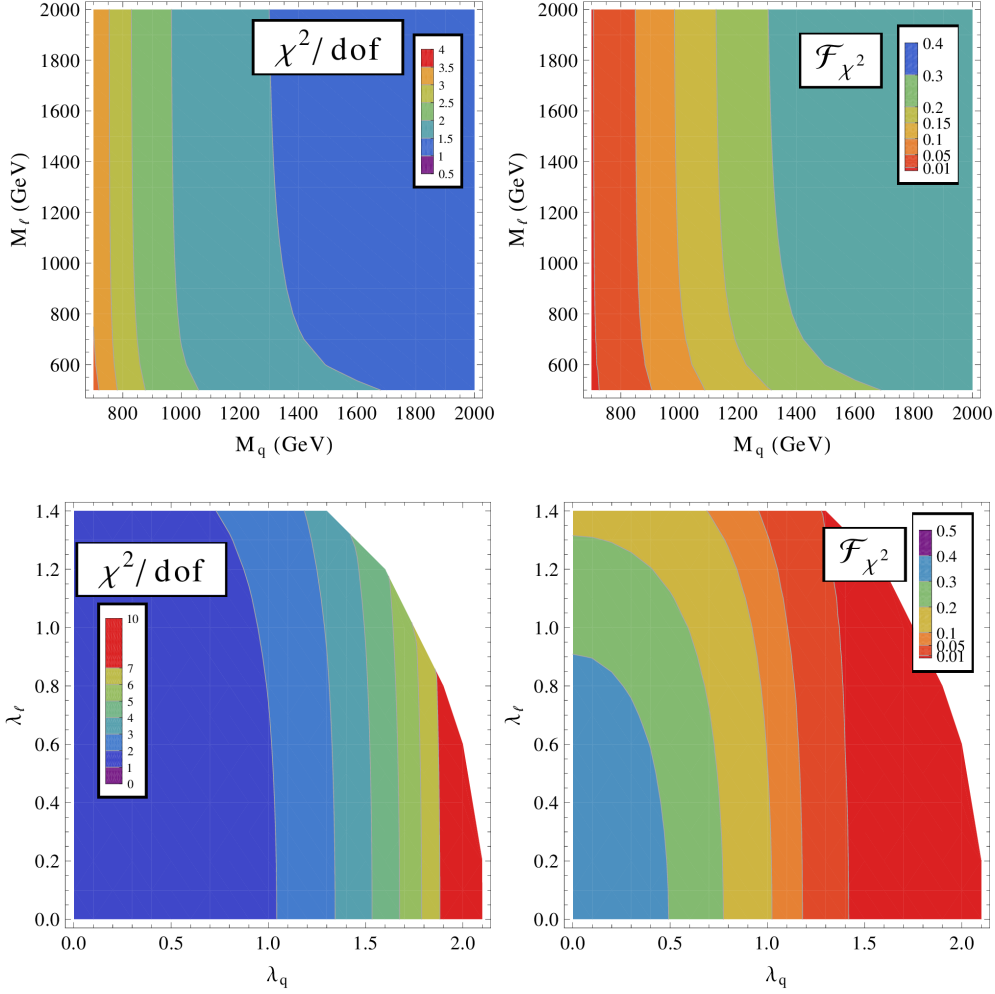


Figure 17: For the VSM₁ model, for $Y_Q = 1/6$, $Y_L = -1/2$, $\lambda_q = 1$, $\lambda_\ell = 1$, $M_q = 1000$ GeV and $M_\ell = 500$ GeV. The colored regions are with all quark mass ≥ 500 GeV, all lepton mass eigenvalues ≥ 250 GeV, and satisfy the S and T constraints at or better than 2σ . In all the plots, χ^2 values decrease and \mathcal{F} values increase as we go toward larger masses, or lower λ .

Acknowledgements: We thank the CERN Theory group for hospitality where this work was initiated. We thank M. Muhlleitner and M. Spira for a discussion on the size of NNLO corrections to the ggh amplitude.

A Gauge boson 2-point functions with vector-like fermions

In a vector-like theory each vertex in Fig. 2 is proportional to $P_L + P_R$, resulting in the total contribution $\Pi_{LL} + \Pi_{LR} + \Pi_{RL} + \Pi_{RR}$. A similar result holds for the derivative Π' also, where $\Pi' = d\Pi/dq^2$. Since we have $\Pi_{LL} = \Pi_{RR}$ and $\Pi_{LR} = \Pi_{RL}$, the above contribution is $2(\Pi_{LL} + \Pi_{LR})$. Using dimensional regularization and continuing to $d = 4 - \epsilon$ dimensions, we have (see for example,

Ref. [91])

$$\Pi_{LL}^{(m_i m_j)}(q^2) = -\frac{4}{(4\pi)^{d/2}} \int_0^1 dx \frac{\Gamma(2-d/2)}{\Delta^{2-d/2}} \left[x(1-x)q^2 - \frac{1}{2}(xm_j^2 + (1-x)m_i^2) \right], \quad (\text{A.71})$$

$$\Pi_{LR}^{(m_i m_j)}(q^2) = -\frac{2}{(4\pi)^{d/2}} \int_0^1 dx \frac{\Gamma(2-d/2)}{\Delta^{2-d/2}} m_i m_j. \quad (\text{A.72})$$

where $\Delta = xm_j^2 + (1-x)m_i^2 - x(1-x)q^2$, and we have dropped terms proportional to $q^\mu q^\nu$ assuming that gauge-bosons connect to massless fermion currents giving zero. We have

$$\lim_{d \rightarrow (4-\epsilon)} \frac{1}{(4\pi)^{d/2}} \frac{\Gamma(2-d/2)}{\Delta^{2-d/2}} = \frac{1}{(4\pi)^2} \left[\frac{2}{\epsilon} - \gamma + \log(4\pi) - \log \Delta \right]. \quad (\text{A.73})$$

For notational ease, in the following we will define $\Pi \equiv \Pi_{LL} + \Pi_{LR}$, similarly for Π' , and also, $\Pi^{\{m_i, m_j\}} = \Pi^{(m_i m_j)} + \Pi^{(m_j m_i)}$, $\Pi^{(m_i)} = \Pi^{(m_i m_i)}$. From Eqs. (A.71), (A.72) and (A.73), we obtain the following

$$\begin{aligned} \Pi^{(m_i m_j)}(0) \Big|_{\text{mass-dep}} &= \frac{1}{32\pi^2} \frac{1}{(m_j^2 - m_i^2)} \{ (m_j^2 - m_i^2)(m_i^2 + m_j^2 - 4m_i m_j) \\ &\quad - 2(m_j^4 \log m_j^2 - m_i^4 \log m_i^2) + 4m_i m_j (m_j^2 \log m_j^2 - m_i^2 \log m_i^2) \}, \\ \Pi^{\{m_i, m_j\}}(0) \Big|_{\text{mass-dep}} &= -\frac{1}{16\pi^2} \frac{1}{(m_j^2 - m_i^2)} \{ 4m_i m_j (m_j^2 - m_i^2) + 2m_j^3 (m_j - 2m_i) \log m_j^2 \\ &\quad + 2m_i^3 (2m_j - m_i) \log m_i^2 + m_i^4 - m_j^4 \}, \\ \Pi^{(m_i)}(0) \Big|_{\text{mass-dep}} &= 0, \end{aligned} \quad (\text{A.74})$$

where ‘‘mass-dep’’ denotes mass dependent finite parts excluding the $2/\epsilon - \gamma + 4\pi$ pieces. Again, from Eqs. (A.71), (A.72) and (A.73), we obtain

$$\begin{aligned} \Pi'_{LR}^{\{m_i, m_j\}}(0) &= -\frac{m_i m_j \left[m_i^4 - m_j^4 - 4m_i^2 m_j^2 \tanh^{-1} \left((m_i^2 - m_j^2)/(m_i^2 + m_j^2) \right) \right]}{8\pi^2 (m_i^2 - m_j^2)^3}, \\ \Pi'_{LL}^{\{m_i, m_j\}}(0) &= -\frac{1}{4\pi^2} \left\{ \frac{1}{3} \left(-\frac{1}{2} + \frac{2}{\epsilon} - \gamma + \log(4\pi) \right) - \frac{1}{18(m_i^2 - m_j^2)^3} (\mathcal{A} - \mathcal{B}) \right\} \\ \mathcal{A} &= (m_i^2 - m_j^2) \left[-5m_i^4 - 5m_j^4 + 22m_i^2 m_j^2 + 6(m_i^2 - m_j^2)^2 \log m_i m_j \right. \\ &\quad \left. + 18(m_i^4 - m_j^4) \operatorname{cosech}^{-1} \left(\frac{2m_i m_j}{m_i^2 - m_j^2} \right) \right] \\ \mathcal{B} &= 12(m_i^2 + m_j^2)(m_i^4 + m_j^4 - m_i^2 m_j^2) \coth^{-1} \left(\frac{m_i^2 + m_j^2}{m_i^2 - m_j^2} \right), \\ \Pi'^{(m)}(0) &= -\frac{2}{3(4\pi)^2} \left[\frac{2}{\epsilon} - \gamma + \log(4\pi) - \log m^2 \right], \end{aligned} \quad (\text{A.75})$$

which are valid for $(m_i \neq m_j)$, and we recall the definition $\Pi' \equiv \Pi'_{LL} + \Pi'_{LR}$. The $\log m^2$ terms are understood to be $\log(m^2/\mu^2)$ where μ is an arbitrary renormalization scale. For our numerical computations we set $\mu = M_Z$, but we have verified that our results remain the same even if a different value of μ is chosen.

B Explicit expressions for the mixing coefficients

This appendix contains expressions for the various coefficients that we defined in order to simplify the formulae in Sec. 4.

Mixing through the Higgs boson

We give here the explicit expressions for the mixing coefficients from section 5 between the new vector-like generation and the SM quarks through the Higgs boson.

As explained in the text, α_{ij} are the new Yukawa couplings that arise from applying the matrices that diagonalise the mass matrix in Eq. (44) to the matrix of Yukawa couplings in the Lagrangian, given in Eq. (51). In order to simplify the expressions derived for α_{ij} , we define the following quantities

$$\begin{aligned}
a_1^u &= (V_L^u)^{12} = \frac{m_{ct}m_{tt} + m_{cc}m_{ct} + m_{cT}m_{tT}}{m_{tt}^2 - m_{cc}^2}, & a_4^u &= (V_R^u)^{12} = \frac{m_{ct}m_{tt} + m_{cc}m_{ct} + \mu_c\mu_t}{m_{tt}^2 - m_{cc}^2} \\
a_2^u &= (V_L^u)^{13} = \frac{\mu_T m_{cT} + \mu_c m_{cc} + \mu_t m_{ct}}{\mu_T^2 - m_{cc}^2}, & a_5^u &= (V_R^u)^{13} = \frac{\mu_T \mu_c + m_{cT}m_{cc} + m_{tT}m_{ct}}{\mu_T^2 - m_{cc}^2} \\
a_3^u &= (V_L^u)^{23} = \frac{\mu_T m_{tT} + \mu_c m_{ct} + \mu_t m_{tt}}{\mu_T^2 - m_{tt}^2}, & a_6^u &= (V_R^u)^{23} = \frac{m_{ct}m_{cT} + \mu_t \mu_T + m_{tt}m_{tT}}{\mu_T^2 - m_{tt}^2}
\end{aligned} \tag{B.76}$$

Similar quantities can be defined for the down type expressions, with

$$\begin{aligned}
a_1^d &= (V_L^d)^{12} = \frac{m_{sb}m_{bb} + m_{ss}m_{sb} + m_{sB}m_{bB}}{m_{bb}^2 - m_{ss}^2}, & a_4^d &= (V_R^d)^{12} = \frac{m_{sb}m_{bb} + m_{ss}m_{sb} + \mu_s\mu_b}{m_{bb}^2 - m_{ss}^2} \\
a_2^d &= (V_L^d)^{13} = \frac{\mu_B m_{sB} + \mu_s m_{ss} + \mu_b m_{sb}}{\mu_B^2 - m_{ss}^2}, & a_5^d &= (V_R^d)^{13} = \frac{\mu_B \mu_s + m_{sB}m_{ss} + m_{bB}m_{sb}}{\mu_B^2 - m_{ss}^2} \\
a_3^d &= (V_L^d)^{23} = \frac{\mu_B m_{bB} + \mu_s m_{sb} + \mu_b m_{bb}}{\mu_B^2 - m_{bb}^2}, & a_6^d &= (V_R^d)^{23} = \frac{m_{sb}m_{sB} + \mu_b \mu_B + m_{bb}m_{bB}}{\mu_B^2 - m_{bb}^2}.
\end{aligned} \tag{B.77}$$

This results in the following coefficients α_{ij} for the up-type matrix

$$\begin{aligned}
\alpha_{cc} &= \lambda_{cc} + \lambda_{tc}(-a_1^u) + (-a_4^u)(\lambda_{ct} + \lambda_{tt}(-a_1^u)) + (-a_5^u)(\lambda_{cT} + \lambda_{tT}(-a_1^u)) \\
\alpha_{ct} &= \lambda_{ct} + \lambda_{tt}(-a_1^u) + a_4^u(\lambda_{cc} + \lambda_{tc}(-a_1^u)) + a_5^u(\lambda_{cT} + \lambda_{tT}(-a_1^u)) \\
\alpha_{cT} &= \lambda_{cT} + \lambda_{tT}(-a_1^u) + a_5^u(\lambda_{cc} + \lambda_{tc}(-a_1^u)) + a_6^u(\lambda_{ct} + \lambda_{tt}(-a_1^u)) \\
\alpha_{tc} &= \lambda_{tc} + \lambda_{cc}a_1^u + (-a_4^u)(\lambda_{tt} + \lambda_{ct}a_1^u) + (-a_5^u)(\lambda_{tT} + \lambda_{cT}a_1^u) \\
\alpha_{tt} &= \lambda_{tt} + \lambda_{ct}a_1^u + a_4^u(\lambda_{tc} + \lambda_{cc}a_1^u) + (-a_6^u)(\lambda_{tT} + \lambda_{cT}a_1^u) \\
\alpha_{tT} &= \lambda_{tT} + \lambda_{cT}a_1^u + a_5^u(\lambda_{tc} + \lambda_{cc}a_1^u) + a_6^u(\lambda_{tt} + \lambda_{ct}a_1^u) \\
\alpha_{Tc} &= \lambda_{tc}a_2^u + \lambda_{cc}a_2^u + (-a_4^u)(\lambda_{tt}a_3^u + \lambda_{ct}a_2^u) + (-a_5^u)(\lambda_{tT}a_3^u + \lambda_{cT}a_2^u) \\
\alpha_{Tt} &= \lambda_{ct}a_2^u + \lambda_{tt}a_3^u + a_4^u(\lambda_{tc}a_3^u + \lambda_{cc}a_2^u) + (-a_6^u)(\lambda_{tT}a_3^u + \lambda_{cT}a_2^u) \\
\alpha_{TT} &= \lambda_{cT}a_2^u + \lambda_{tT}a_3^u + a_6^u(\lambda_{tt}a_3^u + \lambda_{ct}a_2^u) + a_5^u(\lambda_{tc}a_3^u + \lambda_{cc}a_2^u)
\end{aligned} \tag{B.78}$$

and similar coefficients for the down type, with $c \leftrightarrow s$, $t \leftrightarrow b$, $T \leftrightarrow B$.

The mass eigenvalues M_i ($i = c, t, T$) are given by the following equations

$$\begin{aligned}
M_c &= m_{cc} - a_1^u m_{tc} - a_2^u \mu_c - a_4^u (m_{ct} - a_1^u m_{tt} - a_2^u \mu_t) - a_5^u (m_{cT} - a_1^u m_{tT} - a_2^u \mu_T) \\
M_t &= m_{tt} + a_1^u m_{ct} - a_3^u \mu_t + a_4^u (m_{tc} + a_1^u m_{cc} - a_3^u \mu_c) - a_6^u (m_{tT} + a_1^u m_{cT} - a_3^u \mu_T) \\
M_T &= \mu_T + a_2^u m_{cT} + a_3^u m_{tT} + a_5^u (\mu_c + a_2^u m_{cc} + a_3^u m_{tc}) + a_6^u (\mu_t + a_2^u m_{ct} + a_3^u m_{tt})
\end{aligned} \tag{B.79}$$

Mixing through the Z boson

The coefficients β_{ij} defined in the text are given here explicitly. They govern the size of mixing between the vector-like and SM quarks via the Z boson discussed in section 5.

$$\begin{aligned}
\beta_{11} &= \frac{1}{2} \left[1 - \left(\frac{\mu_T m_{cT} + \mu_c m_{cc} + \mu_t m_{ct}}{m_{cc}^2 - \mu_T^2} \right)^2 \right] - \frac{2}{3} \sin^2 \theta_W \\
\beta_{12} &= -\frac{1}{2} \left(\frac{\mu_T m_{cT} + \mu_c m_{cc} + \mu_t m_{ct}}{m_{cc}^2 - \mu_T^2} \right) \left(\frac{\mu_T m_{tT} + \mu_c m_{ct} + \mu_t m_{tt}}{m_{tt}^2 - \mu_T^2} \right) \\
\beta_{13} &= -\frac{1}{2} \left(\frac{\mu_T m_{cT} + \mu_c m_{cc} + \mu_t m_{ct}}{m_{cc}^2 - \mu_T^2} \right) \\
\beta_{21} &= -\frac{1}{2} \left(\frac{\mu_T m_{cT} + \mu_c m_{cc} + \mu_t m_{ct}}{m_{cc}^2 - \mu_T^2} \right) \left(\frac{\mu_T m_{tT} + \mu_c m_{ct} + \mu_t m_{tt}}{m_{tt}^2 - \mu_T^2} \right) \\
\beta_{22} &= \frac{1}{2} \left[1 - \left(\frac{\mu_T m_{tT} + \mu_c m_{ct} + \mu_t m_{tt}}{m_{tt}^2 - \mu_T^2} \right)^2 \right] - \frac{2}{3} \sin^2 \theta_W \\
\beta_{23} &= -\frac{1}{2} \left(\frac{\mu_T m_{tT} + \mu_c m_{ct} + \mu_t m_{tt}}{m_{tt}^2 - \mu_T^2} \right) \\
\beta_{31} &= -\frac{1}{2} \left(\frac{\mu_T m_{cT} + \mu_c m_{cc} + \mu_t m_{ct}}{m_{cc}^2 - \mu_T^2} \right) \\
\beta_{32} &= -\frac{1}{2} \left(\frac{\mu_T m_{tT} + \mu_c m_{ct} + \mu_t m_{tt}}{m_{tt}^2 - \mu_T^2} \right) \\
\beta_{33} &= -\frac{2}{3} \sin^2 \theta_W
\end{aligned} \tag{B.80}$$

Similar expressions can be found for the down-type quark interactions with the Z, but are not listed here.

References

- [1] T. P. T. Dijkstra, L. R. Huiszoon and A. N. Schellekens, Nucl. Phys. B **710**, 3 (2005) [hep-th/0411129].
- [2] O. Lebedev, H. P. Nilles, S. Raby, S. Ramos-Sanchez, M. Ratz, P. K. S. Vaudrevange and A. Wingerter, Phys. Lett. B **645**, 88 (2007) [hep-th/0611095];
- [3] S. Raby and A. Wingerter, Phys. Rev. Lett. **99**, 051802 (2007) [arXiv:0705.0294 [hep-ph]].
- [4] B. A. Dobrescu and C. T. Hill, Phys. Rev. Lett. **81**, 2634 (1998) [hep-ph/9712319].
- [5] R. S. Chivukula, B. A. Dobrescu, H. Georgi and C. T. Hill, Phys. Rev. D **59**, 075003 (1999) [hep-ph/9809470].
- [6] H. -J. He, T. M. P. Tait and C. P. Yuan, Phys. Rev. D **62**, 011702 (2000) [hep-ph/9911266].
- [7] S. Gopalakrishna, T. Mandal, S. Mitra and G. Moreau, arXiv:1306.2656 [hep-ph].
- [8] R. Contino, L. Da Rold and A. Pomarol, Phys. Rev. D **75**, 055014 (2007) [hep-ph/0612048].

- [9] C. Anastasiou, E. Furlan and J. Santiago, Phys. Rev. D **79**, 075003 (2009) [arXiv:0901.2117 [hep-ph]].
- [10] N. Vignaroli, JHEP **1207**, 158 (2012) [arXiv:1204.0468 [hep-ph]].
- [11] A. De Simone, O. Matsedonskyi, R. Rattazzi and A. Wulzer, JHEP **1304**, 004 (2013) [arXiv:1211.5663 [hep-ph]].
- [12] C. Delaunay, C. Grojean and G. Perez, JHEP **1309**, 090 (2013) [arXiv:1303.5701 [hep-ph]].
- [13] M. Gillioz, R. Grober, A. Kapuvari and M. Muhlleitner, JHEP **1403**, 037 (2014) [arXiv:1311.4453 [hep-ph]].
- [14] T. Han, H. E. Logan, B. McElrath and L. -T. Wang, Phys. Rev. D **67**, 095004 (2003) [hep-ph/0301040].
- [15] M. S. Carena, J. Hubisz, M. Perelstein and P. Verdier, Phys. Rev. D **75**, 091701 (2007) [hep-ph/0610156].
- [16] S. Matsumoto, T. Moroi and K. Tobe, Phys. Rev. D **78**, 055018 (2008) [arXiv:0806.3837 [hep-ph]].
- [17] J. Berger, J. Hubisz and M. Perelstein, JHEP **1207**, 016 (2012) [arXiv:1205.0013 [hep-ph]].
- [18] J. Kang, P. Langacker and B. D. Nelson, Phys. Rev. D **77**, 035003 (2008) [arXiv:0708.2701 [hep-ph]].
- [19] S. P. Martin, Phys. Rev. D **81**, 035004 (2010) [arXiv:0910.2732 [hep-ph]].
- [20] P. W. Graham, A. Ismail, S. Rajendran and P. Saraswat, Phys. Rev. D **81**, 055016 (2010) [arXiv:0910.3020 [hep-ph]].
- [21] S. P. Martin, Phys. Rev. D **82**, 055019 (2010) [arXiv:1006.4186 [hep-ph]].
- [22] T. Moroi, R. Sato and T. T. Yanagida, Phys. Lett. B **709**, 218 (2012) [arXiv:1112.3142 [hep-ph]].
- [23] S. P. Martin and J. D. Wells, Phys. Rev. D **86**, 035017 (2012) [arXiv:1206.2956 [hep-ph]].
- [24] W. Fischler and W. Tangarife, arXiv:1310.6369 [hep-ph].
- [25] M. Endo, K. Hamaguchi, S. Iwamoto and N. Yokozaki, Phys. Rev. D **85**, 095012 (2012) [arXiv:1112.5653 [hep-ph]]; M. Endo, K. Hamaguchi, K. Ishikawa, S. Iwamoto and N. Yokozaki, JHEP **1301**, 181 (2013) [arXiv:1212.3935 [hep-ph]].
- [26] F. del Aguila and M. J. Bowick, Nucl. Phys. B **224**, 107 (1983).
- [27] F. del Aguila, M. Perez-Victoria and J. Santiago, JHEP **0009**, 011 (2000) [hep-ph/0007316].
- [28] F. del Aguila, J. de Blas and M. Perez-Victoria, Phys. Rev. D **78**, 013010 (2008) [arXiv:0803.4008 [hep-ph]].
- [29] J. Kearney, A. Pierce and N. Weiner, Phys. Rev. D **86**, 113005 (2012) [arXiv:1207.7062 [hep-ph]].

- [30] See, for example, N. Bonne and G. Moreau, Phys. Lett. B **717**, 409 (2012) [arXiv:1206.3360 [hep-ph]].
- [31] N. Arkani-Hamed, K. Blum, R. T. D’Agnolo and J. Fan, JHEP **1301**, 149 (2013) [arXiv:1207.4482 [hep-ph]].
- [32] S. Gopalakrishna, T. Mandal, S. Mitra and R. Tibrewala, Phys. Rev. D **84**, 055001 (2011) [arXiv:1107.4306 [hep-ph]].
- [33] D. Carmi, A. Falkowski, E. Kufflik and T. Volansky, arXiv:1202.3144 [hep-ph].
- [34] A. Joglekar, P. Schwaller and C. E. M. Wagner, JHEP **1212**, 064 (2012) [arXiv:1207.4235 [hep-ph]].
- [35] M. Fairbairn and P. Grothaus, JHEP **1310**, 176 (2013) [arXiv:1307.8011 [hep-ph]].
- [36] S. Dawson and E. Furlan, Phys. Rev. D **86**, 015021 (2012) [arXiv:1205.4733 [hep-ph]].
- [37] S. Fajfer, A. Greljo, J. F. Kamenik and I. Mustac, JHEP **1307**, 155 (2013) [arXiv:1304.4219 [hep-ph]].
- [38] J. A. Aguilar-Saavedra, EPJ Web Conf. **60**, 16012 (2013) [arXiv:1306.4432 [hep-ph]].
- [39] S. Dawson, E. Furlan and I. Lewis, Phys. Rev. D **87**, 014007 (2013) [arXiv:1210.6663 [hep-ph]].
- [40] G. Moreau, Phys. Rev. D **87**, 015027 (2013) [arXiv:1210.3977 [hep-ph]].
- [41] S. Choi, S. Jung and P. Ko, JHEP **1310**, 225 (2013) [arXiv:1307.3948].
- [42] A. Azatov, O. Bondu, A. Falkowski, M. Felcini, S. Gascon-Shotkin, D. K. Ghosh, G. Moreau and S. Sekmen, arXiv:1204.0455 [hep-ph].
- [43] K. Harigaya, S. Matsumoto, M. M. Nojiri and K. Tobioka, Phys. Rev. D **86**, 015005 (2012) [arXiv:1204.2317 [hep-ph]].
- [44] G. Cacciapaglia, A. Deandrea, D. Harada and Y. Okada, JHEP **1011**, 159 (2010) [arXiv:1007.2933 [hep-ph]]; G. Cacciapaglia, A. Deandrea, L. Panizzi, N. Gaur, D. Harada and Y. Okada, JHEP **1203**, 070 (2012) [arXiv:1108.6329 [hep-ph]]; M. Buchkremer, G. Cacciapaglia, A. Deandrea and L. Panizzi, Nucl. Phys. B **876**, 376 (2013) [arXiv:1305.4172 [hep-ph]].
- [45] J. A. Aguilar-Saavedra, R. Benbrik, S. Heinemeyer and M. Prez-Victoria, Phys. Rev. D **88**, no. 9, 094010 (2013) [arXiv:1306.0572 [hep-ph]].
- [46] R. Dermisek and A. Raval, Phys. Rev. D **88**, 013017 (2013) [arXiv:1305.3522 [hep-ph]].
- [47] F. S. Queiroz and W. Shepherd, arXiv:1403.2309 [hep-ph].
- [48] A. K. Alok and S. Gangal, Phys. Rev. D **86**, 114009 (2012) [arXiv:1209.1987 [hep-ph]]; A. K. Alok, S. Banerjee, D. Kumar and S. U. Sankar, arXiv:1402.1023 [hep-ph].
- [49] A. Falkowski, D. M. Straub and A. Vicente, arXiv:1312.5329 [hep-ph].
- [50] T. K. Hemmick, D. Elmore, T. Gentile, P. W. Kubik, S. L. Olsen, D. Ciampa, D. Nitz and H. Kagan *et al.*, Phys. Rev. D **41**, 2074 (1990).

- [51] T. Yamagata, Y. Takamori and H. Utsunomiya, *Phys. Rev. D* **47**, 1231 (1993).
- [52] G. D. Starkman, A. Gould, R. Esmailzadeh and S. Dimopoulos, *Phys. Rev. D* **41**, 3594 (1990).
- [53] D. Fargion and M. Khlopov, *Grav. Cosmol.* **19**, 219 (2013) [hep-ph/0507087].
- [54] G. D. Mack, J. F. Beacom and G. Bertone, *Phys. Rev. D* **76**, 043523 (2007) [arXiv:0705.4298 [astro-ph]]; G. D. Mack and A. Manohar, *J. Phys. G* **40**, 115202 (2013).
- [55] N. E. Mavromatos, arXiv:1111.1563 [hep-ph].
- [56] M. Reece, *New J. Phys.* **15**, 043003 (2013) [arXiv:1208.1765 [hep-ph]].
- [57] M. -L. Xiao and J. -H. Yu, arXiv:1404.0681 [hep-ph].
- [58] H. Davoudiasl, I. Lewis and E. Ponton, *Phys. Rev. D* **87**, 093001 (2013) [arXiv:1211.3449 [hep-ph]].
- [59] M. Baak, M. Goebel, J. Haller, A. Hoecker, D. Ludwig, K. Moenig, M. Schott and J. Stelzer, *Eur. Phys. J. C* **72**, 2003 (2012) [arXiv:1107.0975 [hep-ph]].
- [60] M. Baak, M. Goebel, J. Haller, A. Hoecker, D. Kennedy, R. Kogler, K. Moenig and M. Schott *et al.*, *Eur. Phys. J. C* **72**, 2205 (2012) [arXiv:1209.2716 [hep-ph]].
- [61] M. Ciuchini, E. Franco, S. Mishima and L. Silvestrini, *JHEP* **1308**, 106 (2013) [arXiv:1306.4644 [hep-ph]].
- [62] A. Dighe, D. Ghosh, R. M. Godbole and A. Prasath, *Phys. Rev. D* **85**, 114035 (2012) [arXiv:1204.3550 [hep-ph]].
- [63] M. E. Peskin and T. Takeuchi, *Phys. Rev. Lett.* **65**, 964 (1990). M. E. Peskin and T. Takeuchi, *Phys. Rev. D* **46**, 381 (1992).
- [64] G. Altarelli and R. Barbieri, *Phys. Lett. B* **253**, 161 (1991); G. Altarelli, R. Barbieri and S. Jadach, *Nucl. Phys. B* **369**, 3 (1992) [Erratum-ibid. B **376**, 444 (1992)].
- [65] I. Maksymyk, C. P. Burgess and D. London, *Phys. Rev. D* **50**, 529 (1994) [hep-ph/9306267].
- [66] L. Lavoura and J. P. Silva, *Phys. Rev. D* **47**, 2046 (1993).
- [67] J. Beringer *et al.* [Particle Data Group Collaboration], *Phys. Rev. D* **86**, 010001 (2012), and 2013 partial update for the 2014 edition.
- [68] G. D. Kribs, T. Plehn, M. Spannowsky and T. M. P. Tait, *Phys. Rev. D* **76**, 075016 (2007) [arXiv:0706.3718 [hep-ph]].
- [69] G. Aad *et al.* [ATLAS Collaboration], arXiv:1307.1427 [hep-ex].
- [70] CMS Collaboration, “Combination of standard model Higgs boson searches and measurements of the properties of the new boson with a mass near 125 GeV“, CMS-PAS-HIG-13-005, 2013.
- [71] [Tevatron Electroweak Working Group and CDF and D0 Collaborations], arXiv:1107.5255 [hep-ex].

- [72] The ATLAS collaboration, ATLAS-CONF-2013-102; CMS Collaboration, CMS-PAS-TOP-13-005.
- [73] M. J. Dugan and L. Randall, Phys. Lett. B **264**, 154 (1991).
- [74] P. Bamert and C. P. Burgess, Z. Phys. C **66**, 495 (1995) [hep-ph/9407203].
- [75] K. Agashe, R. Contino, L. Da Rold and A. Pomarol, Phys. Lett. B **641**, 62 (2006) [hep-ph/0605341].
- [76] <http://cds.cern.ch/record/1557571/files/B2G-12-015-pas.pdf>
- [77] <http://cds.cern.ch/record/1525525/files/ATLAS-CONF-2013-018.pdf>
- [78] M. Buchkremer and A. Schmidt, Adv. High Energy Phys. **2013** (2013) 690254 [Adv. High Energy Phys. **2013** (2013) 690254] [arXiv:1210.6369 [hep-ph]].
- [79] S. Chatrchyan *et al.* [CMS Collaboration], Phys. Lett. B **713** (2012) 408 [arXiv:1205.0272 [hep-ex]].
- [80] B. Acharya *et al.* [MoEDAL Collaboration], arXiv:1405.7662 [hep-ph].
- [81] CMS Collaboration [CMS Collaboration], CMS-PAS-HIG-13-034.
- [82] S. Chatrchyan *et al.* [CMS Collaboration], arXiv:1312.4194 [hep-ex].
- [83] CMS Collaboration [CMS Collaboration], CMS NOTE NOTE-13-002
- [84] E. Furlan, JHEP **1110**, 115 (2011) [arXiv:1106.4024 [hep-ph]].
- [85] S. Gori and I. Low, JHEP **1309**, 151 (2013) [arXiv:1307.0496 [hep-ph]].
- [86] A. Djouadi, Phys. Rept. **457**, 1 (2008) [hep-ph/0503172].
- [87] M. Spira, A. Djouadi, D. Graudenz and P. M. Zerwas, Nucl. Phys. B **453**, 17 (1995) [hep-ph/9504378].
- [88] A. Djouadi and A. Lenz, Phys. Lett. B **715**, 310 (2012) [arXiv:1204.1252 [hep-ph]].
- [89] L. Lyons, “Statistics For Nuclear And Particle Physicists,” Cambridge, Uk: Univ. Pr. (1986) 226p.
- [90] J. Baglio, A. Djouadi and R. M. Godbole, Phys. Lett. B **716**, 203 (2012) [arXiv:1207.1451 [hep-ph]].
- [91] M. E. Peskin and D. V. Schroeder, “An Introduction to quantum field theory,” Reading, USA: Addison-Wesley (1995) 842 p.